Journal of Geosciences, 54 (2009), 221–243 DOI: 10.3190/jgeosci.048

Original paper

Tourmalinites in the metamorphic complex of the Svratka Unit (Bohemian Massif): a study of compositional growth of tourmaline and genetic relations

Renata ČOPJAKOVÁ[1,2*], David BURIÁNEK[1], Radek ŠKODA[1,2], Stanislav HOUZAR[3]

[1] *Czech Geological Survey, Leitnerova 23, 658 59 Brno, Czech Republic; copjakova@sci.muni.cz*
[2] *Institute of Geological Sciences, Masaryk University, Kotlářská 2, 611 37 Brno, Czech Republic*
[3] *Department of Mineralogy and Petrography, Moravian Museum, Zelný trh 6, 659 37 Brno, Czech Republic*
[*] *Corresponding author*

Tourmalinites (rocks with an association Tu + Qtz + Ms ± Grt ± Bt ± Ky ± Sil ± Pl ± Kfs) from the Svratka Unit form stratiform layers hosted in mica schists. The chemical composition of tourmaline from tourmalinites varies from Al-rich schorl to dravite. The tourmaline usually exhibits three compositional domains, which are, from centre to the rim: a chemically inhomogeneous brecciated core (zone I), a volumetrically minor internal rim zone II, and a dominant outermost zone III.

The compositional variability of tourmaline in all the zones is controlled by the $(^{X}\square\,^{Y}Al\,^{W}OH)$ $(^{X}Na\,^{Y}Mg\,^{W}F)_{-1}$ and $^{Y}Fe^{Y}Mg_{-1}$ substitutions. The tourmaline of the zone I corresponds to highly vacanced X-site, Al-rich schorl with lower F (up to 0.43 apfu), which is interpreted as an older, low-temperature hydrothermal tourmaline. Tourmaline of the zone II corresponds to dravite rich in F (reaching up to 0.66 apfu) crystallizing during the prograde metamorphism. Lastly, the Al-rich schorl–dravite of the zone III grew most likely during retrograde metamorphism.

The tourmaline from the host mica schists has a similar chemical composition. The central dravite part corresponds to the zone II, and the predominant schorl–dravite rim to the zone III, in tourmalines from tourmalinites. Overall, the dravite exhibits compositional characteristics of the prograde, amphibolite-facies metamorphic event characterised by the mineral assemblage Qtz + Ms + Bt + Tu ± Ky ± St ± Grt. The second generation of tourmaline (schorl–dravite), as well as the rim of garnets present in both the mica schists and tourmalinites, formed during exhumation of the Svratka Unit accompanied by decreasing pressure and temperature. In the mica schists, this event resulted in decompression breakdown of staurolite, according to the reaction St + Ms + Qtz = Grt + Sil + Bt + H_2O. Breakdown of muscovite could have released B and F used for tourmaline formation. The P-T conditions of this retrograde metamorphism were calculated at 600–640 °C and 5–6 kbar.

Tourmalinites are interpreted as a part of a metamorphosed volcano-sedimentary complex primarily rich in F and B, however, the derivation of all the F- and B-rich fluids from the neighbouring migmatites and metagranites is unlikely. Similarities in the chemical composition of the tourmalinites and the mica schists suggest a similar protolith to both rock types. The variation in most of the elements reflects the mineral composition associated with the transition from mica schist to tourmalinite.

Keywords: tourmalinite, mica schist, schorl, dravite, metamorphism, B- and F-rich fluids, Svratka Unit
Received: 11 March 2009; accepted 19 March 2009; handling editor: M. Novák
The online version of this article (doi: 10.3190/jgeosci.048) contains supplementary electronic material

1. Introduction

Tourmalinites are known from numerous metamorphic sequences around the world, and their origin is most commonly interpreted by one of the following processes:

(1) Interaction of metapelites and B-rich hydrothermal/magmatic or metamorphic fluids (Appel 1985; Plimer 1988; Slack et al. 1993; Slack 1996);

(2) Metamorphism of B-rich exhalites or evaporites (Abraham et al. 1972; Slack et al. 1984; Chown 1987);

(3) Metamorphism of detrital tourmaline accumulations derived from tourmaline-rich source rocks, for example B-rich granites (Henry and Dutrow 1996, 1997).

However, more genetic scenarios are theoretically possible (Slack 1996).

Regardless their exact genesis, studying the tourmalinites may clearly contribute to knowledge of metamorphic and/or magmatic B-rich fluids and could also provide data for lithostratigraphic correlations (Slack et al. 1993; Henry and Dutrow 1997).

Tourmalinites occur in several geological units of the Bohemian Massif. Kebrt et al. (1984) and Lhotský (1982) described tourmalinite layers enclosed in gneisses in the Varied Unit of the Moldanubian Zone north of Jindřichův Hradec. Tourmalinites hosted in mica schists are present in the Krkonoše–Jizera Unit, near Žacléřské Boudy and

Smrčí in the Krkonoše Mts. and near Nové Město pod Smrkem in the Jizera Mts. (Vašák 1981; Rambousek 1983). In the Krušné Mts. area, tourmalinites occur near Tisová in a sequence of phyllites, meta-tuffites and metabasites and in the Měděnec area hosted in mica schists (Kebrt et al. 1984; Pertold et al. 1994; Šrein et al. 1997).

Tourmalinite layers hosted in mica schists are abundant in the Svratka Unit but their nature and genesis have been little studied so far. The occurrences of such tourmalinites in the Svratka Unit (SU) were first reported by Veselý (1969); synoptic characterization was published by Kebrt et al. (1984). These authors considered the pre-metamorphic origin of boron and interpreted the tourmalinites as syngenetic rocks without any relationship to tourmaline metagranites common in the southern part of the SU. Tourmalinites in the studied area were focal point for geological prospection for boron (Páša and Hranáč 1994).

The tourmalinites from Pernštejn underwent retrograde regional metamorphism at P > 3–4 kbar and T > 400–500 °C, which produced tourmaline-rich quartz segregations (Qtz + Tu ± Ms ± Ky ± And ± Pl) (Houzar et al. 1997, 1998). Tourmaline of both paragenetic types (the tourmalinites and the tourmaline-rich quartz segregations) corresponds to intermediate members of the schorl–dravite series, with an elevated F content in some places (Houzar et al. 1997, 1998).

The purpose of this paper is to report new petrographic, mineral and whole-rock chemical data from the tourmalinites and associated mica schists of the Svratka Unit, constrain their genesis and to contribute to the ongoing discussion of processes leading to the formation of these intriguing F- and B-rich rocks.

2. Geological setting

The studied region is situated in the southern and central parts of the Svratka Unit near the border with the Moldanubian Zone, the Moravian Dome and the Polička Unit (Bohemian Massif). The area is built by medium- to coarse-grained mica schists, paragneisses, migmatites, F-, Sn- and B-rich orthogneisses, coarse-grained porphyritic metagranites, amphibolites, serpentinites and rare marbles (Němec 1979, 1986; Melka et al. 1992; Houzar et al. 1997, 2006; Buriánek et al. 2009). Tourmaline is a common mineral in this area (Němec 1979; Pertoldová 1986; Novotná 1987; Novák et al. 1998; Čopjaková et al. 2007; Buriánek and Čopjaková 2008). It forms disseminated grains in mica schists and gneisses, whereas in migmatites it is typically concentrated in tourmaline-rich layers or nodules. Tourmalinites occur in conformable layers and boudins in garnet-muscovite mica schist and muscovite mica schist, predominantly in the southern part of the Svratka Unit.

Several phases of metamorphism were recognized within the SU (Buriánek et al. 2006). Relics of the oldest HP-HT metamorphism (M_1 ~12 kbar) were reported from skarns (Pertoldová et al. 1998; Blažková 2005; Pertoldová et al. this volume). The conditions of regional metamorphism (M_2) of the SU were estimated at ~ 640–670 ºC and 6–8 kbar (Tajčmanová et al. 2005). This metamorphic event was recorded especially in mica schists by the stable mineral assemblage Ms + Bt + Grt + St + Ky (Tajčmanová et al. 2005; Buriánek and Čopjaková 2008). The presence of latter formed sillimanite aggregates is probably associated with a retrograde metamorphic event (M_3) at ~ 580–650 °C and 5–6 kbar (Buriánek and Čopjaková 2008; Buriánek et al. 2009). Chlorite partially replaced garnet and biotite as a result of retrogression during exhumation of the SU.

3. Methods

Tourmalinites and the surrounding mica schists were taken from outcrops or slope debris in the southern and central parts of the SU at localities Borovnice, Jimramov, Kozlov, Ujčov, Kovářová, Nedvědice–North, Nedvědice–South, Pernštejn, as well as at Rožná at contact between the SU and the Moldanubian Zone, and near Tišnov at Klucanina Hill (Klucanina Group) (for sample locations, see Tab. 1 and Fig. 1).

The mineral compositions were determined using the Cameca SX 100 electron microprobe at the Joint Laboratory of Electron Microscopy and Microanalysis of the Masaryk University and the Czech Geological Survey in Brno. Operating conditions for analyses were as follows: an accelerating voltage of 15 kV, a beam current of 10 nA for tourmaline, feldspar, mica, and 20 nA for garnet; a beam diameter of 5 μm for tourmaline, feldspar and mica, and <1 μm for garnet. Natural and synthetic standards were used (Si, Al – sanidine; Mg – olivine; Fe – almandine; Ca – andradite; Mn – rhodonite; Ti – Ti-hornblende; Cr – chromite; Na – albite; K – orthoclase; P – apatite; F – topaz; Cl, V – vanadinite; Zn – gahnite; Cu- metallic Cu; Y – YAG). The raw concentration data were corrected using the method of Pouchou and Pichoir (1985).

The tourmaline group is represented by the general formula $XY_3Z_6T_6O_{18}(BO_3)_3V_3W$ (Hawthorne and Henry 1999), where X = Na, Ca, □, K; Y = Mg, Fe^{2+}, Al, Fe^{3+}, Li, Mn, Ti^{4+}, Cr^{3+}, Zn, V^{3+}; Z = Al, Mg, Fe^{3+}, Cr^{3+}, V^{3+}; T = Si, Al, B; B = B; V = OH, O; W = OH, F, O. Tourma-

⇨

Fig. 1 Schematic geological map of the Svratka Unit with sample locations (modified according to Melichar et al. 2004; Mrázová and Otava 2005; Hanžl and Vít 2005; Buriánek et al. 2006; Hanžl et al. 2006).

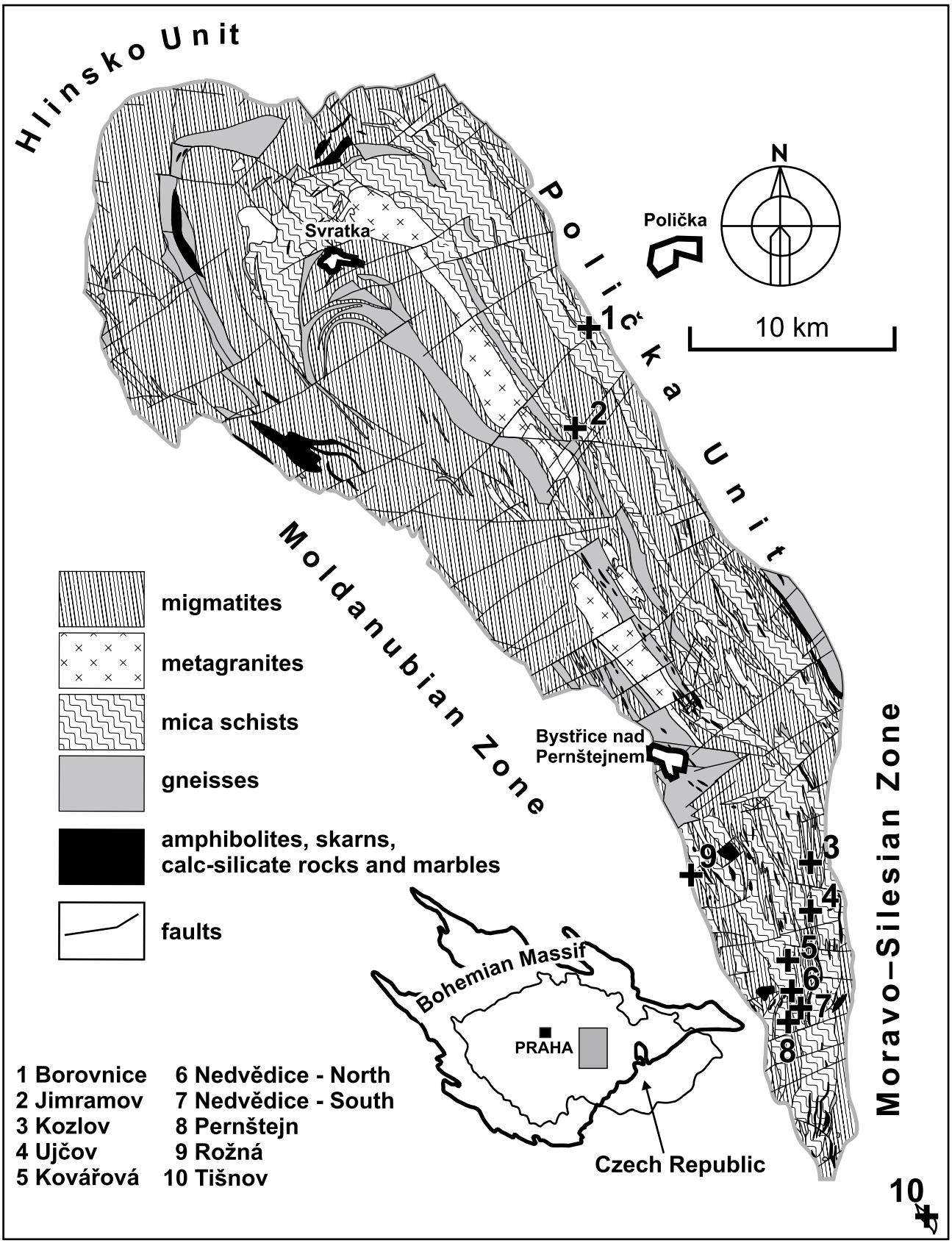
Hlinsko Unit
Polička Unit
Moldanubian Zone
Moravo–Silesian Zone
Svratka
Polička
Bystřice nad Pernštejnem
N
10 km
migmatites
metagranites
mica schists
gneisses
amphibolites, skarns, calc-silicate rocks and marbles
faults
Bohemian Massif
PRAHA
Czech Republic
1 Borovnice
2 Jimramov
3 Kozlov
4 Ujčov
5 Kovářová
6 Nedvědice - North
7 Nedvědice - South
8 Pernštejn
9 Rožná
10 Tišnov

Tab. 1 The list of samples studied by EMPA with mineral assemblages. Mineral abbreviations according to Kretz (1983)

No.	locality	rock type	mineral assemblage	GPS location
1	Borovnice	mica schist	Qtz + Ms + Bt + Grt + Sill + Pl	49°40'35.157"N, 16°11'12.132"E
2	Jimramov	tourmalinite	Tu + Qtz + Grt + Bt + Ms	49°37'26.747"N, 16°12'22.323"E
3	Kozlov	tourmalinite	Tu + Qtz + Ms + Bt + Grt + Ky + Pl	49°30'21.985"N, 16°19'09.176"E
4	Kozlov	tourmalinite	Tu + Qtz + Ms	
5	Kozlov	mica schist	Qtz + Ms + Tu + Pl	
6	Kozlov	mica schist	Qtz + Ms + Bt + Tu + Grt + Sill + Pl	
7	Ujčov	tourmalinite	Tu + Qtz + Bt	49°29'37.847"N, 16°19'29.068"E
8	Kovářová	tourmalinite	Tu + Qtz + Grt + Ms + Bt	49°28'04.438"N, 16°18'56.537"E
9	Nedvědice–North	tourmalinite	Tu + Qtz + Grt + Ms	49°27'53.940"N, 16°18'57.051"E
10	Nedvědice–North	mica schist	Qtz + Ms + Bt + Tu	
11	Nedvědice–North	mica schist	Qtz + Ms + Tu	
12	Nedvědice–South	tourmalinite	Tu + Qtz + Grt + Bt + Ky + Sill	49°27'33.267"N, 16°19'15.176"E
13	Nedvědice–South	mica schist	Qtz + Ms + Bt + Grt + St	
14	Nedvědice–South	mica schist	Qtz + Pl + Bt + Ms + Sill + Tu	
15	Pernštejn	tourmalinite	Tu + Qtz + Ms + Ky	49°27'05.022"N, 16°18'41.634"E
16	Pernštejn	mica schist	Qtz + Ms + Bt + Grt + Sill + Pl	
17	Pernštejn	mica schist	Qtz + Ms + Bt + Grt + Sill	
18	Rožná	tourmalinite	Tu + Qtz + Ms + Bt + Pl + Kfs	49°29'31.709"N, 16°14'17.901"E
19	Tišnov	tourmalinite	Tu + Qtz + Ms + Bt + Grt + Pl	49°20'42.815"N, 16°26'04.882"E
20	Tišnov	mica schist	Qtz + Ms + Bt + Grt + Tu + Pl	

line was normalized on the basis of 31 anions assuming the presence of all Fe as Fe^{2+}. The procedure assumes the total B = 3 and OH + F = 4 atoms per formula unit (apfu), although OH + F < 4 is very likely.

Mica formulae were obtained on the basis of 12 anions, all Fe is reported as Fe^{2+} and the water content was recalculated according to the relation OH + F + Cl = 2 apfu. The garnet formulae were normalized on the basis of 12 oxygen atoms, Fe^{2+} and Fe^{3+} amounts were assessed according to the ideal stoichiometry and charge-valence calculation.

The THERMOCALC program v. 2.7 was employed for the calculation of the P-T conditions in the metapelites. It was run in the average P-T mode using the data set and activities from the AX program (Holland and Powell 1998).

The whole-rock major- and trace-element analyses were determined in the Acme Analytical Laboratories, Ltd., Vancouver, Canada. Major oxides were analysed by the ICP-MS method. Loss on ignition (LOI) was calculated from the weight difference after ignition at 1 000 ºC. The REE and other trace elements were analyzed by INAA and ICP-MS following $LiBO_2$ fusion. The geochemical data were recalculated using the GCDkit software package (Janoušek et al. 2006).

4. Geological position and petrography of tourmalinites and associated mica schists

4.1. Geological position of tourmalinites

The studied tourmalinites form stratiform layers or lens-shaped bodies of variable thickness (<1 cm to up to 1 m) commonly enclosed in mica schists, but their outcrops are relatively rare. The tourmalinites are often found as debris in the southern part of the Svratka Unit near the villages of Pernštejn, Kovářová, Ujčov and Kozlov (Fig. 1). These occurrences indicate that they form a N–S trending discontinuous belt, which continues near the border with the Polička Unit near Jimramov. An isolated

⇨

Fig. 2 Tourmalinites in Back-Scattered Electron (BSE) images. **a –** Large tourmaline crystal with highlighted zones I–III; **b –** Tourmaline from the Kozlov locality; **c –** Tourmaline from Kovářová; **d –** Detailed image of a small schorl core in tourmaline from Rožná; **e –** Tourmaline without core, Rožná; **f –** Tourmaline with inner dravite core and highlighted tourmaline zones I–III, Tišnov; **g –** Garnet enclosing quartz and tourmaline from the Nedvědice–South; **h –** Tourmaline grains enclosed in kyanite, Nedvědice–South. The symbols for rock-forming minerals are after Kretz (1983).

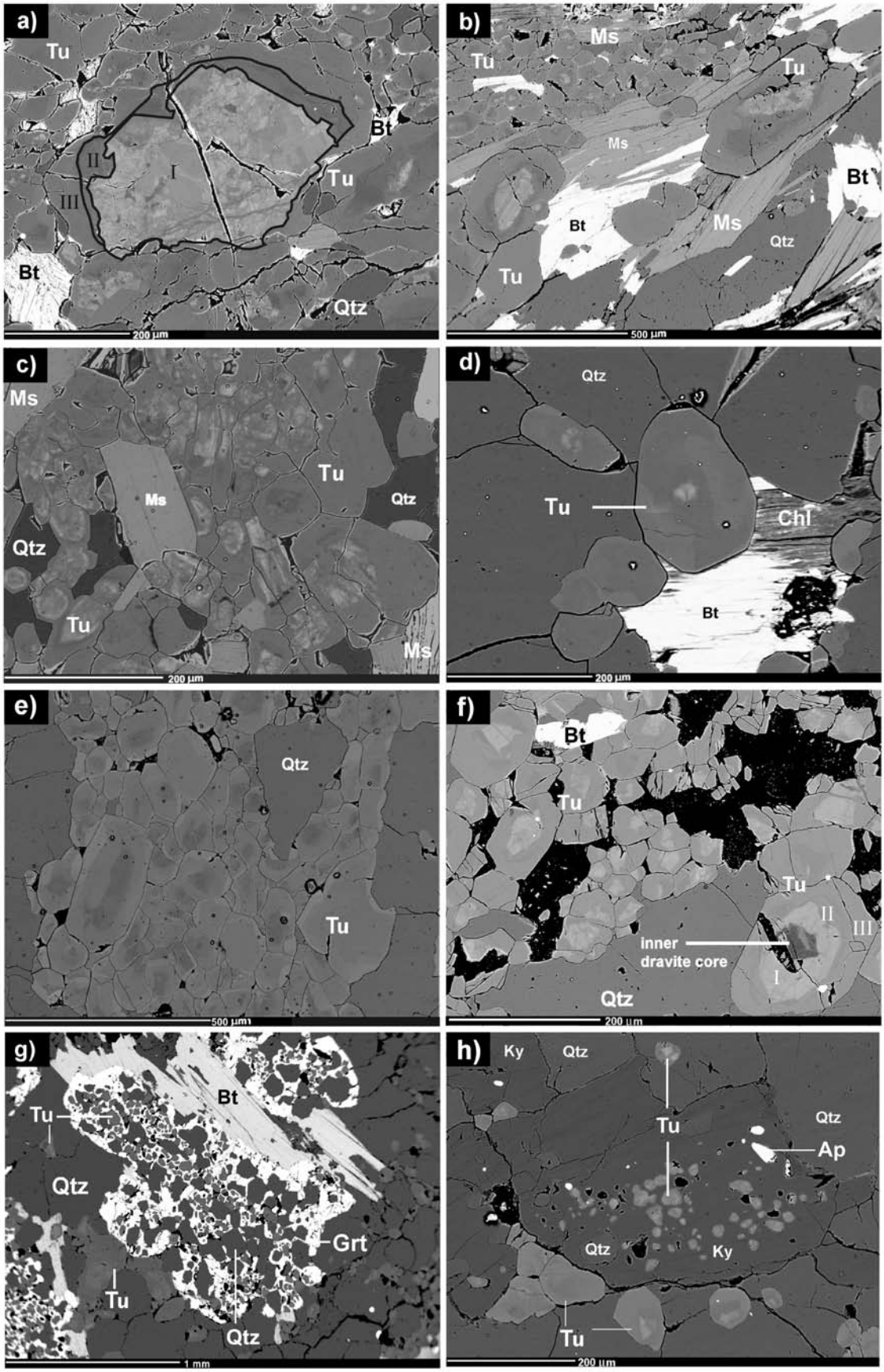
a)
Tu
Bt
II
I
III
Tu
Bt
Qtz
200 µm
b)
Ms
Tu
Tu
Ms
Bt
Bt
Ms
Qtz
Tu
500 µm
c)
Ms
Tu
Ms
Qtz
Qtz
Tu
Ms
200 µm
d)
Qtz
Tu
Chl
Bt
200 µm
e)
Qtz
Tu
500 µm
f)
Bt
Tu
Tu
II
III
inner
dravite core
I
Qtz
200 µm
g)
Bt
Tu
Qtz
Grt
Tu
Qtz
1 mm
h)
Ky
Qtz
Tu
Qtz
Ap
Qtz
Ky
Tu
200 µm

Tab. 2 Representative chemical compositions of tourmaline from tourmalinites and mica schists

	tourmalinites												
	Jimramov			Kozlov			Ujčov		Kovářová			Nedvědice–S	
	zone I	zone II	zone III	zone I	zone II	zone III	zone I	zone III	zone I	zone II	zone III	zone I	zone III
	1	2	3	4	5	6	7	8	9	10	11	12	13
SiO_2	36.16	37.36	36.04	35.42	36.36	34.85	34.55	36.73	35.59	37.19	36.42	35.98	36.94
TiO_2	0.64	0.46	0.70	0.89	0.32	0.84	0.70	0.81	0.88	0.54	0.81	0.56	0.59
Al_2O_3	32.25	32.11	33.05	31.04	31.39	31.43	35.11	31.37	33.55	32.99	33.58	32.46	32.44
Cr_2O_3	0.00	0.03	0.00	0.00	0.03	0.00	0.00	0.00	0.00	0.00	0.00	0.00	0.03
V_2O_3	n.a.	n.a.	n.a.	0.04	0.00	0.00	0.00	0.10	0.05	0.04	0.04	0.00	0.06
FeO	14.08	8.61	10.93	15.00	7.89	12.99	10.92	7.07	12.48	7.26	7.78	13.77	9.08
MnO	0.10	0.00	0.00	0.10	0.07	0.08	0.00	0.00	0.00	0.04	0.00	0.00	0.00
MgO	2.14	6.05	4.13	2.29	6.80	3.39	2.78	7.15	2.19	6.44	5.39	1.78	5.45
CaO	0.08	0.19	0.64	0.04	0.45	0.62	0.53	0.37	0.30	0.06	0.48	0.04	0.13
Na_2O	2.06	2.29	1.95	2.52	2.56	2.40	1.99	2.34	1.60	2.41	1.95	1.55	2.13
K_2O	0.04	0.04	0.03	0.08	0.00	0.07	0.04	0.00	0.03	0.03	0.05	0.06	0.13
F	0.45	0.84	0.59	0.81	1.27	0.88	0.14	0.37	0.00	0.16	0.13	0.21	0.47
Cl	n.a.	n.a.	n.a.	0.00	0.00	0.00	0.00	0.00	0.00	0.00	0.00	0.00	0.00
B_2O_3*	10.46	10.70	10.60	10.35	10.53	10.32	10.52	10.60	10.46	10.76	10.67	10.35	10.66
H_2O*	3.40	3.29	3.38	2.29	2.12	2.25	3.56	3.48	3.61	3.64	3.62	3.47	3.45
O=F	-0.19	-0.35	-0.25	-0.34	-0.53	-0.37	-0.06	-0.16	0.00	-0.07	-0.05	-0.09	-0.20
O=Cl	0.00	0.00	0.00	0.00	0.00	0.00	0.00	0.00	0.00	0.00	0.00	0.00	0.00
Total	101.67	101.62	101.79	100.66	99.26	99.76	100.88	100.24	100.76	101.49	100.87	100.15	101.36
n.a. – not analyzed													
* Calculated on the basis of ideal stoichiometry (B = 3 apfu; OH + F + Cl = 4 apfu)													
T site													
Si^{4+}	6.008	6.066	5.908	5.951	5.999	5.866	5.710	6.020	5.911	6.007	5.931	6.040	6.024
Al^{3+}	0.000	0.000	0.092	0.049	0.001	0.134	0.276	0.000	0.086	0.000	0.069	0.000	0.000
Y Z site													
Al^{3+}	6.315	6.145	6.293	6.097	6.103	6.101	6.563	6.059	6.481	6.280	6.376	6.422	6.235
Ti^{4+}	0.080	0.056	0.086	0.112	0.040	0.106	0.087	0.100	0.110	0.066	0.099	0.071	0.072
Cr^{3+}	0.000	0.004	0.000	0.000	0.004	0.000	0.000	0.000	0.000	0.000	0.000	0.000	0.004
V^{3+}	n.a.	n.a.	n.a.	0.005	0.000	0.000	0.000	0.013	0.007	0.005	0.005	0.000	0.008
Fe^{2+}	1.956	1.169	1.498	2.107	1.089	1.829	1.509	0.969	1.733	0.981	1.060	1.933	1.238
Mn^{2+}	0.014	0.000	0.000	0.014	0.010	0.011	0.000	0.000	0.000	0.005	0.000	0.000	0.000
Mg^{2+}	0.530	1.465	1.009	0.574	1.673	0.851	0.685	1.747	0.542	1.551	1.309	0.445	1.325
subtotal	8.895	8.839	8.886	8.909	8.919	8.898	8.844	8.888	8.873	8.888	8.849	8.871	8.882
X site													
Ca^{2+}	0.014	0.033	0.112	0.007	0.080	0.112	0.094	0.065	0.053	0.010	0.084	0.007	0.023
Na^{+}	0.664	0.721	0.620	0.821	0.819	0.783	0.638	0.744	0.515	0.755	0.616	0.505	0.673
K^{+}	0.008	0.008	0.006	0.017	0.000	0.015	0.008	0.000	0.006	0.006	0.010	0.013	0.027
X-vacancy	0.314	0.238	0.262	0.155	0.101	0.090	0.260	0.191	0.426	0.229	0.290	0.475	0.277
OH^{-}	3.764	3.569	3.694	3.570	3.337	3.532	3.927	3.808	4.000	3.918	3.933	3.889	3.758
F^{-}	0.236	0.431	0.306	0.430	0.663	0.468	0.073	0.192	0.000	0.082	0.067	0.111	0.242
Cl^{-}	n.a.	n.a.	n.a.	0.000	0.000	0.000	0.000	0.000	0.000	0.000	0.000	0.000	0.000
B^{3+}	3.000	3.000	3.000	3.000	3.000	3.000	3.000	3.000	3.000	3.000	3.000	3.000	3.000
O^{2-}	30.764	30.569	30.694	30.570	30.337	30.532	30.927	30.808	31.000	30.918	30.933	30.889	30.758
catsum	18.590	18.668	18.626	18.772	18.817	18.809	18.585	18.716	18.449	18.666	18.558	18.437	18.630
ansum	31.000	31.000	31.000	31.000	31.000	31.000	31.000	31.000	31.000	31.000	31.000	31.000	31.000
Mg/(Mg+Fe)	0.213	0.556	0.402	0.214	0.606	0.318	0.312	0.643	0.238	0.613	0.553	0.187	0.517

	tourmalinites										mica schists			
	Pernštejn			Rožná			Tišnov				Kozlov		Nedvědice–S	Tišnov
	zone I	zone II	zone III	zone I	zone II	zone III	in core	zone I	zone II	zone III	core			
	14	15	16	17	18	19	20	21	22	23	24	25	26	27
SiO_2	35.52	36.01	36.23	36.35	37.36	36.54	38.46	35.61	36.80	36.68	37.72	36.70	36.96	35.79
TiO_2	0.38	0.47	0.64	0.07	0.13	0.67	0.18	0.04	0.72	0.71	0.46	0.81	0.51	0.94
Al_2O_3	35.67	32.86	33.48	32.53	33.25	32.64	32.27	30.59	30.84	32.47	32.15	32.25	33.91	30.86
Cr_2O_3	0.04	0.00	0.04	0.00	0.00	0.00	0.00	0.01	0.00	0.02	0.00	0.01	0.00	0.00
V_2O_3	0.05	0.04	0.09	0.00	0.00	0.00	0.01	0.02	0.05	0.06	0.05	0.06	0.02	0.09
FeO	9.40	7.88	8.52	11.07	4.88	6.18	0.76	12.55	6.56	7.42	4.80	8.19	8.65	11.15
MnO	0.00	0.00	0.00	0.05	0.00	0.00	0.00	0.04	0.00	0.00	0.00	0.00	0.00	0.00
MgO	3.58	6.08	5.10	3.44	7.49	7.06	10.65	3.58	7.10	6.12	8.60	5.71	4.89	5.11
CaO	0.52	0.33	0.29	0.03	0.10	0.26	0.16	0.20	0.42	0.30	0.06	0.35	0.32	0.49
Na_2O	1.56	2.10	2.05	2.03	2.41	2.51	2.50	1.93	2.45	2.08	2.62	2.26	1.65	2.52
K_2O	0.05	0.06	0.05	0.00	0.00	0.04	0.01	0.06	0.02	0.02	0.00	0.04	0.24	0.07
F	0.50	0.94	0.76	0.31	0.50	0.45	0.76	0.35	0.50	0.42	0.14	0.52	0.72	0.46
Cl	0.00	0.00	0.00	0.00	0.00	0.00	0.00	0.00	0.00	0.00	0.00	0.00	0.00	0.00
B_2O_3*	10.65	10.57	10.63	10.41	10.74	10.66	10.88	10.17	10.52	10.61	10.82	10.62	10.73	10.47
H_2O*	3.44	3.20	3.31	3.44	3.47	3.46	3.39	3.34	3.39	3.46	3.67	3.42	2.44	3.39
O=F	-0.21	-0.40	-0.32	-0.13	-0.21	-0.19	-0.32	-0.15	-0.21	-0.18	-0.06	-0.22	-0.30	-0.19
O=Cl	0.00	0.00	0.00	0.00	0.00	0.00	0.00	0.00	0.00	0.00	0.00	0.00	0.00	0.00
Total	101.14	100.14	100.87	99.60	100.12	100.28	99.77	98.38	99.28	100.23	101.11	100.73	100.73	101.15
n.a. - not analyzed														
* Calculated on the basis of ideal stoichiometry (B = 3 apfu; OH + F + Cl = 4 apfu)														
T site														
Si^{4+}	5.799	5.923	5.925	6.069	6.046	5.959	6.142	6.084	6.081	6.006	6.059	6.007	5.986	5.940
Al^{3+}	0.201	0.077	0.075	0.000	0.000	0.041	0.000	0.000	0.000	0.000	0.000	0.000	0.014	0.060
Y Z site														
Al^{3+}	6.662	6.293	6.377	6.401	6.342	6.233	6.074	6.159	6.006	6.266	6.086	6.222	6.459	5.977
Ti^{4+}	0.047	0.058	0.079	0.009	0.016	0.082	0.022	0.005	0.089	0.087	0.056	0.100	0.062	0.117
Cr^{3+}	0.005	0.000	0.005	0.000	0.000	0.000	0.000	0.001	0.000	0.003	0.000	0.001	0.000	0.000
V^{3+}	0.007	0.005	0.012	0.000	0.000	0.000	0.001	0.003	0.007	0.008	0.006	0.008	0.003	0.012
Fe^{2+}	1.283	1.084	1.165	1.546	0.660	0.843	0.102	1.793	0.907	1.016	0.645	1.121	1.172	1.548
Mn^{2+}	0.000	0.000	0.000	0.007	0.000	0.000	0.000	0.006	0.000	0.000	0.000	0.000	0.000	0.000
Mg^{2+}	0.871	1.491	1.243	0.856	1.807	1.717	2.536	0.912	1.749	1.494	2.059	1.393	1.181	1.264
subtotal	8.875	8.931	8.881	8.819	8.825	8.875	8.735	8.879	8.758	8.874	8.852	8.845	8.877	8.918
X site														
Ca^{2+}	0.091	0.058	0.051	0.005	0.017	0.045	0.027	0.037	0.074	0.053	0.010	0.061	0.056	0.087
Na^{+}	0.494	0.670	0.650	0.657	0.756	0.794	0.774	0.639	0.785	0.660	0.816	0.717	0.518	0.811
K^{+}	0.010	0.013	0.010	0.000	0.000	0.008	0.002	0.013	0.004	0.004	0.000	0.008	0.050	0.015
X-vacancy	0.405	0.259	0.289	0.338	0.227	0.153	0.197	0.311	0.137	0.283	0.174	0.214	0.376	0.087
OH^{-}	3.742	3.511	3.607	3.836	3.744	3.768	3.616	3.811	3.739	3.783	3.929	3.731	3.631	3.759
F^{-}	0.258	0.489	0.393	0.164	0.256	0.232	0.384	0.189	0.261	0.217	0.071	0.269	0.369	0.241
Cl^{-}	0.000	0.000	0.000	0.000	0.000	0.000	0.000	0.000	0.000	0.000	0.000	0.000	0.000	0.000
B^{3+}	3.000	3.000	3.000	3.000	3.000	3.000	3.000	3.000	3.000	3.000	3.000	3.000	3.000	3.000
O^{2-}	30.742	30.511	30.607	30.836	30.744	30.768	30.616	30.811	30.739	30.782	30.929	30.731	30.631	30.759
catsum	18.470	18.672	18.592	18.550	18.645	18.722	18.686	18.656	18.717	18.601	18.747	18.640	18.498	18.831
ansum	31.000	31.000	31.000	31.000	31.000	31.000	31.000	31.000	31.000	31.000	31.000	31.000	31.000	31.000
Mg/(Mg+Fe)	0.404	0.579	0.516	0.356	0.732	0.671	0.961	0.337	0.659	0.595	0.761	0.554	0.502	0.45

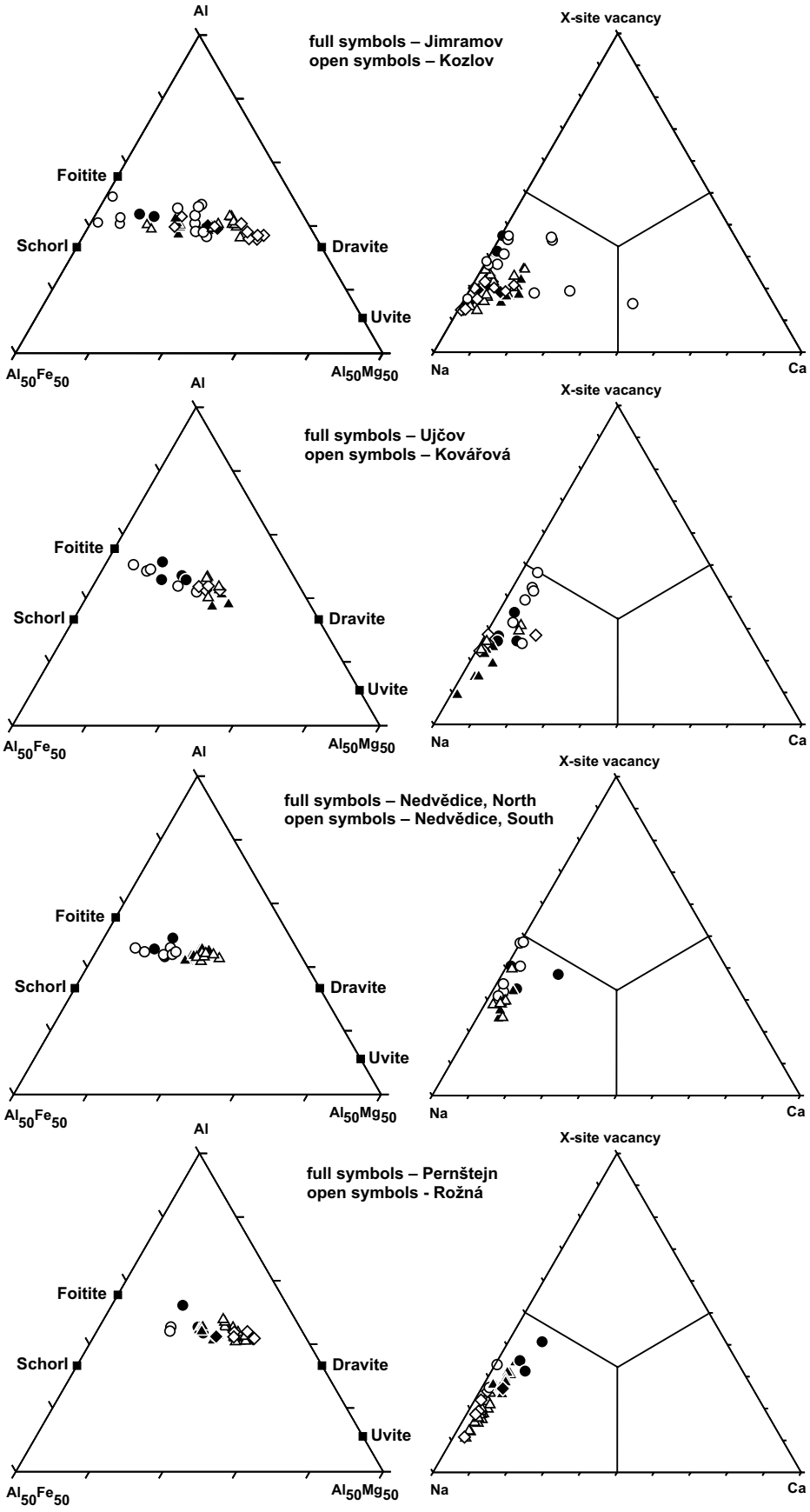

outcrop of the tourmalinites was found at Rožná, at the boundary with the Moldanubian Zone. Lastly, relatively thin tourmalinite layers (0.5–10 cm) in mica schists are encountered near Tišnov at the foot of Klucanina Hill (Klucanina Group). The Klucanina Group forms isolated enclaves of mica schists, migmatites and blue Nedvědice marbles belonging to the SU (Houzar and Novák 2006) along the boundary between the Svratka Dome (Moravo-Silesian Zone) and the Boskovice Furrow. The thickness and frequency of tourmalinites in the SU decrease towards the north. Field observations do not provide any direct clue helping to assess the relationship of tourmalinites to metagranites and migmatites, but tourmaline-bearing migmatites commonly occur in the proximity of tourmalinites. However, the tourmalinites are typically associated with Nedvědice marbles, which form thin, up to 40 m thick layers underlying metapelites and migmatites in the SU, and at Tišnov as well.

4.2. Petrography of tourmalinites and associated mica schists

The tourmalinites usually have a relatively simple mineral assemblage. They predominantly consist of preferentially oriented elongated tourmaline and quartz. The tourmaline contents vary from 15

Fig. 3 Chemical composition of tourmaline from tourmalinites of the Svratka Unit plotted in Al – $Al_{50}Mg_{50}$ – $Al_{50}Fe_{50}$ and X-site vacancy – Na – Ca ternary diagrams. Symbols: circles – zone I, diamonds – zone II, triangles – zone III.

to 70 vol. %. Minor minerals include muscovite, garnet and, in some samples, also biotite, kyanite, sillimanite, plagioclase and K-feldspar. Feldspars usually occur in small pegmatoidal lenses (Qtz + Kfs + Pl + Ms). Accessory minerals include apatite (in places it reaches 10 vol. %, though), rutile, ilmenite, and rarely also zircon with monazite.

Two-mica schists grading to muscovite schists and two-mica schists with sillimanite and garnet, all with abundant columnar tourmaline, represent the typical country-rock of tourmalinites. The modal amounts of plagioclase vary. Minor to accessory minerals include kyanite, staurolite, apatite, zircon and monazite. The mineral association (Qtz + Ms ± Bt ± Grt ± Sil ± Ky ± Pl ± Tu ± St) and rock structure are characteristic of mica schists in the whole Svratka Unit. Staurolite occurs typically only in mica schists of the northern part of the SU. In mica schists of the central and southern parts of the SU (approximately south of the Svratka–Polička line) staurolite occurs only occasionally as small inclusions in garnet or quartz or in quartz lenses (for more details see Buriánek and Čopjaková 2008). The mineral assemblages of the individual tourmalinite and mica schist samples are listed in Tab. 1.

5. Mineralogy and chemical composition of tourmalinites and their host rocks

5.1. Tourmaline

5.1.1. Tourmaline in tourmalinites

Tourmaline in the tourmalinites forms euhedral to subhedral preferentially oriented crystals. Three tourmaline zones were distinguished in the BSE images and under the optical microscope: the core (zone I) with strong blue–grey pleochroism, an internal rim of the core (zone II) with pale–brown pleochroism and the outermost zone (zone III) with brown pleochroism. A detailed BSE image of a large tourmaline crystal with highlighted individual zones I–III is shown in Fig. 2a. Patchy zoning in tourmaline cores was observed under the optical microscope and in the BSE images. The number and size of tourmaline cores decrease from the northern localities (Jimramov, Kozlov, Ujčov, Kovářová) (Fig. 2b–c) to the south and west, i.e. towards the boundary with the Moldanubian Zone. The cores are relatively abundant, but very small, in samples from Pernštejn, and occur only occasionally at Rožná (Fig. 2d–e). Tourmaline cores are also abundant and relatively large in tourmalinites near Tišnov (Fig. 2f), similar to those from the Kozlov or Jimramov localities. Tourmaline cores are anhedral, brecciated and rehealed, and enclosed in younger tourmaline of the zone II. Small tourmaline grains composed of the core (zone I) rehealed and rimmed by a narrow zone II are typically enclosed in garnet, kyanite, biotite or muscovite (Fig. 2g–h).

Representative analyses of tourmaline from different zones are presented in Tab. 2. Chemical compositions of tourmaline from tourmalinites in the SU are plotted in Fig. 3 and those from the Klucanina Group in Fig. 4a.

Tourmaline – Zone I. The chemical composition of the cores corresponds to Al-rich schorl with high X-site vacancy (Tab. 2). The Z-site is fully occupied by Al. Relatively high Al contents at the Y-site (0.19–0.66 apfu) are typical, with an exception of a rarely found Ca-rich core in the tourmaline from Kozlov, with Al contents at the Y-site close to zero. The Fe contents at the Y-site of 1.15–2.54 apfu Fe are the highest of all three zones. The tourmaline cores exhibit a wide variations in Fe and Mg with X_{Mg} [molar Mg/(Mg + Fe)] varying in a range of 0.03–0.53. The Ti contents vary from 0.3–1.0 wt. % TiO_2 (0.01–0.16 Ti apfu). The X-site is predominantly occupied by Na, with the elevated X-site vacancy ranging from 0.17 to 0.46 pfu. The Ca content is often slightly elevated, corresponding to 0.5–0.9 wt. % CaO (0.09–0.15 Ca apfu); at Kozlov it scarcely reaches up to 2.6 wt. % CaO (0.46 Ca apfu). The fluorine contents in the Fe-rich cores attain 0.43 apfu but in some cases they are below the detection limit of the electron microprobe.

Moreover, some tourmaline grains from the tourmalinites of Tišnov contain a small inner core enclosed by a schorl of zone I, dark in BSE image (Fig. 2f). These inner cores, together with the schorl host, are crushed and healed by the tourmaline of the zone II. The inner core corresponds to almost pure dravite (X_{Mg} = 0.94–0.96, Al = 6.05–6.19 apfu, X-site vacancy = 0.12–0.26 pfu) with the highest F content (~0.4 apfu) of all the zones in tourmaline of the Tišnov tourmalinites (see Tab. 2).

Tourmaline – Zone II. Tourmaline of the zone II overgrows the core (zone I) and fills cracks in it. In the fine-grained tourmalinites, these zones are too narrow for electron microprobe analysis. On the other hand, this zone is most evolved in the relatively coarse-grained tourmalinites (Kozlov, Jimramov and Rožná localities), mainly in tourmaline grains, which are not enclosed by other rock-forming minerals. The tourmaline of this zone corresponds to dravite. Although the Al contents are the lowest of all three zones, the Z-site is usually fully occupied by Al and up to 0.37 apfu Al still enters the Y-site. Typical of this zone is high and variable Mg (1.29–2.15 apfu) at the Y-site, with X_{Mg} varying from 0.51 to 0.78. The titanium contents are low, close to 0.4 wt. % TiO_2 (0.05 Ti apfu). Dravite is characterized by low, but variable, X-site vacancies (0.10–0.28 pfu) and very low Ca (usually below 0.06 apfu, 0.3 wt. % CaO). The tourmaline of this zone attains the highest F contents (up to 0.66 apfu, 1.27 wt. % F).

Tourmaline – Zone III. The outermost zone of the tourmaline crystals, predominating by volume, represents a relatively homogeneous schorl–dravite composition in the individual samples but the average X_{Mg} (0.30–0.71) varies significantly. In all the diagrams, its composition falls between tourmaline of zone I and tourmaline of zone II (Figs 3–4). The Z-site is usually fully occupied by Al, and up to 0.45 Al apfu enters the Y-site. The titanium contents are low to moderate (0.18–0.91 wt. % TiO_2, 0.02–0.11 apfu). Sodium predominates at the X-site, with a moderate X-site vacancy (0.10–0.39 pfu). The calcium amount does not exceed 0.13 apfu. The fluorine contents vary from 0.05 to 0.50 apfu. The outer zone exhibits weak zoning with a decrease in Mg at the Y-site, increasing Fe, and an increase in vacancies at the expense of Na at the X-site toward the tourmaline rim.

5.1.2. Tourmaline in associated mica schists

Tourmaline in mica schists forms euhedral columnar porphyroblasts up to 5 cm long and 1 cm in diameter. Its modal amount varies significantly, from an accessory to the major rock-forming mineral. It often encloses other rock-forming minerals as muscovite, biotite, garnet and quartz (see Fig. 5a–b). Representative analyses of tourmaline from mica schists are presented in Tab. 2. Chemical compositions of tourmaline from mica schists are plotted in Fig. 4b. This tourmaline corresponds to Al-rich schorl–dravite passing to foitite (Al = 6.09–6.70 apfu, Na = 0.45–0.84 apfu, and X_{Mg} values range from 0.22 to 0.66). It usually exhibits evident continuous zoning (Mg decreases and Fe increases rimwards). A zonal rim is locally present with an increase in Fe and Al accompanied by a decrease in Mg and Na towards rim (Fig. 5a–b). Oscillatory zoned tourmaline grains were also recorded (Fig. 5c). Chemically homogeneous cores free of inclusions, corresponding to dravite (Al = 5.98–6.26 apfu, Na = 0.66–0.82 apfu, X_{Mg} = 0.66–0.77), are rare. Variable, usually moderate to high F contents (0.13–0.60 apfu) are typical of the tourmaline in mica schists, except rare cores with low F (below 0.08 apfu).

5.1.3. Substitution mechanisms

Although the chemical composition of tourmaline from the tourmalinites varies significantly from Al-rich schorl to dravite, similar trends were observed for all three zones in all the studied crystals. A decrease in Al at the Y-site is accompanied by a decrease in X-site vacancy, Fe at the Y-site, as well as an increase in Na at the X-site and Mg at the Y-site (Fig. 6) in all three tourmaline zones. Elevated F contents (reaching up to 0.6 apfu) are typical of all the studied tourmalinites, exhibiting F inversely correlated with Fe. The highest F contents are always in zone II and the lowest in the schorl core (zone I), except for the Tišnov tourmalinite, in which

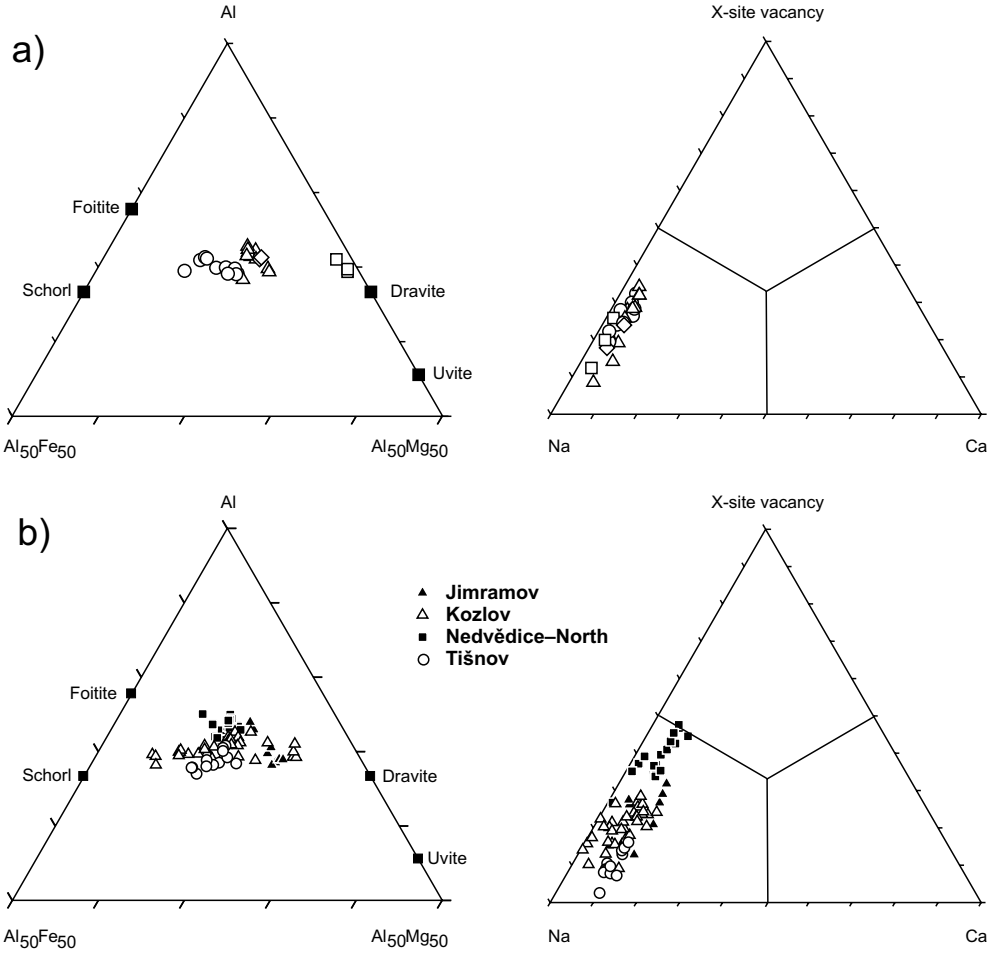

Fig. 4 Chemical composition of tourmaline plotted in Al – $Al_{50}Mg_{50}$ – $Al_{50}Fe_{50}$ and X-site vacancy – Na – Ca ternary diagrams. **a –** Tourmalinites from Tišnov; the same symbols as in Fig. 3 plus open squares – the inner dravite core; **b** – Tourmalines from mica schists.

Tab. 3 Representative chemical compositions of muscovite in tourmalinites and mica schists from following localities: 1 Jimramov, 2 Kozlov, 3 Ujčov, 4 Kovářová, 5 Nedvědice-north, 6 Pernštejn, 7 Rožná, 8 Tišnov, 9 Kozlov, 10 Nedvědice–North, 11 Nedvědice–South, 12 Pernštejn, 13 Tišnov

	tourmalinites								mica schists				
	1	**2**	**3**	**4**	**5**	**6**	**7**	**8**	**9**	**10**	**11**	**12**	**13**
SiO_2	47.36	46.45	46.70	46.70	46.48	46.81	46.48	47.18	46.81	47.12	46.22	46.46	48.27
TiO_2	0.64	0.00	2.30	0.45	0.83	0.77	1.37	2.06	0.40	0.66	0.64	0.40	0.77
Al_2O_3	34.28	36.83	33.02	34.92	34.99	33.29	34.66	27.09	30.63	35.09	35.04	35.14	30.72
Cr_2O_3	0.00	0.00	0.11	0.00	0.05	0.00	0.00	0.00	0.00	0.00	0.00	0.00	0.00
FeO	2.01	0.88	1.07	1.33	1.64	1.45	1.02	4.25	4.32	0.77	0.84	1.41	2.32
MnO	0.03	0.00	0.00	0.00	0.00	0.00	0.00	0.07	0.08	0.00	0.00	0.00	0.00
MgO	0.88	0.42	0.93	0.76	0.75	1.38	0.84	2.95	1.08	0.97	0.50	0.71	1.79
BaO	0.11	0.12	0.20	0.06	0.20	0.20	0.11	0.00	0.00	0.15	0.18	0.25	0.13
K_2O	9.68	8.56	9.80	9.57	9.31	9.93	9.66	10.84	10.65	9.67	9.62	9.69	9.80
Na_2O	0.79	1.95	0.85	1.12	1.10	0.79	0.79	0.05	0.38	0.77	1.26	1.08	0.74
F	1.24	0.19	0.24	0.20	0.34	1.28	0.44	0.87	2.36	1.54	0.15	0.21	1.04
Cl	0.00	0.00	0.00	0.00	0.00	0.00	0.00	0.00	0.00	0.00	0.00	0.00	0.00
H_2O *	3.94	4.46	4.38	4.41	4.36	3.87	4.30	3.96	3.26	3.80	4.41	4.41	3.97
O=F	-0.52	-0.08	-0.10	-0.08	-0.14	-0.54	-0.19	-0.37	-0.99	-0.65	-0.06	-0.09	-0.44
O=Cl	0.00	0.00	0.00	0.00	0.00	0.00	0.00	0.00	0.00	0.00	0.00	0.00	0.00
Total	100.44	99.78	99.58	99.44	99.90	99.24	99.48	98.95	98.98	99.90	98.86	99.71	99.11
* Calculated on the basis of ideal stoichiometry (OH + F + Cl = 2 apfu)													
Si^{4+}	3.133	3.064	3.115	3.108	3.086	3.138	3.092	3.237	3.202	3.116	3.093	3.092	3.245
Ti^{4+}	0.032	0.000	0.115	0.023	0.041	0.039	0.069	0.106	0.021	0.033	0.032	0.020	0.039
Al^{3+}	2.673	2.863	2.596	2.739	2.738	2.631	2.717	2.191	2.469	2.735	2.764	2.756	2.434
Cr^{3+}	0.000	0.000	0.006	0.000	0.003	0.000	0.000	0.000	0.000	0.000	0.000	0.000	0.000
Fe^{2+}	0.111	0.049	0.060	0.074	0.091	0.081	0.057	0.244	0.247	0.043	0.047	0.078	0.130
Mn^{2+}	0.002	0.000	0.000	0.000	0.000	0.000	0.000	0.004	0.005	0.000	0.000	0.000	0.000
Mg^{2+}	0.087	0.041	0.092	0.075	0.074	0.138	0.083	0.302	0.110	0.096	0.050	0.070	0.179
Ba^{2+}	0.003	0.003	0.005	0.002	0.005	0.005	0.003	0.000	0.000	0.004	0.005	0.007	0.003
K^+	0.817	0.720	0.834	0.813	0.788	0.850	0.820	0.949	0.929	0.816	0.821	0.823	0.840
Na^+	0.101	0.249	0.110	0.145	0.142	0.102	0.102	0.007	0.050	0.099	0.164	0.139	0.096
F^-	0.259	0.040	0.051	0.042	0.071	0.270	0.093	0.189	0.511	0.322	0.032	0.044	0.221
Cl^-	0.000	0.000	0.000	0.000	0.000	0.002	0.000	0.000	0.000	0.000	0.000	0.000	0.000
OH^-	1.741	1.960	1.949	1.958	1.929	1.727	1.907	1.811	1.489	1.678	1.968	1.956	1.779
O^{2-}	11.741	11.960	11.949	11.958	11.929	11.727	11.907	11.811	11.489	11.678	11.968	11.956	11.779
catsum	6.958	6.989	6.938	6.978	6.968	6.984	6.942	7.039	7.033	6.941	6.980	6.988	6.968
ansum	12.000	12.000	12.000	12.000	12.000	12.000	12.000	12.000	12.000	12.000	12.000	12.000	12.000

the highest F contents are in the inner dravite core. A positive correlation between Fe and Mg at the Y-site has been observed (Fig. 6). This suggests a heterovalent substitution $^{X}\square\,^{Y}Al\,^{W}OH\,^{X}Na_{-1}\,^{Y}Mg_{-1}\,^{W}F_{-1}$ and a homovalent substitution $^{Y}Fe^{Y}Mg_{-1}$. The same substitutions were observed in the tourmaline from the surrounding mica schists.

Calcium is typically the highest in the schorl core and the lowest in the tourmaline of the zone II. Only a negative correlation of Ca and Na in the outer zone III is evident. The relatively low Ca content makes prediction of a reliable substitution mechanism for Ca at the X-site difficult. Only the rare tourmaline core with variable and anomalously high Ca (0.03–0.47 apfu) exhibits positive correlation of Ca with Mg and negative correlation of Ca with ^{Y}Al, Na and X-site vacancies.

5.2. Associated micas and garnets

Muscovite from the tourmalinites and associated mica schists contains relatively high paragonite (usually 9–25 mol. % and 5–17 mol. % respectively), and phengite components (usually 8–23 mol. % and 10–36 mol. % respectively). Representative analyses of muscovite are presented in Tab. 3. The F contents in muscovite from tourmalinites range from 0.17 to 1.25 wt. % (up to 0.27 apfu) and those from the mica schists are yet higher (0.15–2.36 wt. %, 0.03–0.51 apfu). Fluorine contents exhibit a positive correlation with the phengite and a negative one with the paragonite components.

Biotites from both the tourmalinites and the surrounding mica schists correspond, with exceptions, to annite with the Mg/(Mg + Fe) ratio varying from 0.23 to 0.51

Tab. 4 Representative chemical compositions of biotite in tourmalinites and mica schists from following localities: 1 Jimramov, 2 Kozlov, 3 Ujčov, 4 Nedvědice–South, 5 Rožná, 6 Tišnov, 7 Kozlov, 8 Nedvědice–North, 9 Nedvědice–South, 10 Pernštejn, 11 Tišnov

	tourmalinites						mica schists				
	1	**2**	**3**	**4**	**5**	**6**	**7**	**8**	**9**	**10**	**11**
SiO_2	35.43	35.36	35.98	35.24	35.22	35.18	35.16	35.19	34.96	35.55	34.98
TiO_2	1.56	1.83	1.94	2.11	2.75	1.52	1.94	2.32	2.54	1.10	2.32
Al_2O_3	18.54	19.41	18.19	19.18	19.44	19.17	18.94	18.68	19.59	20.76	18.94
Cr_2O_3	0.00	0.00	0.06	0.00	0.00	0.00	0.05	0.00	0.05	0.00	0.00
FeO	26.30	21.95	20.05	24.27	19.36	21.10	24.65	21.60	21.50	19.97	23.49
MnO	0.20	0.09	0.06	0.00	0.29	0.25	0.29	0.00	0.12	0.00	0.11
MgO	4.82	8.16	9.37	6.04	8.39	8.03	5.70	7.58	7.48	9.00	6.39
BaO	0.13	0.00	0.09	0.00	0.13	0.00	0.07	0.11	0.12	0.00	0.10
K_2O	8.81	8.91	9.51	8.84	9.42	9.03	9.14	9.27	8.78	8.93	8.98
Na_2O	0.18	0.36	0.22	0.41	0.27	0.33	0.27	0.27	0.26	0.50	0.28
F	1.69	0.51	0.55	0.64	0.74	0.84	1.30	1.41	0.18	0.36	0.98
Cl	0.04	0.00	0.00	0.00	0.00	0.00	0.00	0.00	0.00	0.00	0.00
H_2O*	3.04	3.69	3.67	3.59	3.58	3.49	3.26	3.21	3.83	3.80	3.41
O=F	-0.71	-0.21	-0.23	-0.27	-0.31	-0.35	-0.55	-0.59	-0.08	-0.15	-0.41
O=Cl	-0.01	0.00	0.00	0.00	0.00	0.00	0.00	0.00	0.00	0.00	0.00
Total	100.09	100.06	99.55	100.09	99.28	98.72	100.35	99.05	99.41	99.82	99.63
* Calculated on the basis of ideal stoichiometry (OH + F + Cl = 2 apfu)											
Si^{4+}	2.759	2.693	2.742	2.711	2.687	2.714	2.716	2.717	2.677	2.683	2.704
Ti^{4+}	0.091	0.105	0.111	0.122	0.158	0.088	0.113	0.135	0.146	0.062	0.135
Al^{3+}	1.702	1.742	1.634	1.739	1.748	1.743	1.724	1.700	1.768	1.847	1.726
Cr^{3+}	0.001	0.000	0.004	0.000	0.000	0.000	0.003	0.000	0.003	0.000	0.000
Fe^{2+}	1.713	1.398	1.278	1.562	1.235	1.361	1.593	1.395	1.377	1.260	1.519
Mn^{2+}	0.013	0.006	0.004	0.000	0.019	0.016	0.019	0.000	0.008	0.000	0.007
Mg^{2+}	0.560	0.927	1.065	0.693	0.954	0.924	0.656	0.872	0.854	1.013	0.736
Ba^{2+}	0.004	0.000	0.003	0.000	0.004	0.000	0.002	0.003	0.004	0.000	0.003
K^+	0.875	0.866	0.925	0.868	0.917	0.889	0.901	0.913	0.858	0.860	0.886
Na^+	0.027	0.053	0.033	0.061	0.040	0.049	0.040	0.040	0.039	0.073	0.042
F^-	0.416	0.123	0.133	0.156	0.179	0.205	0.318	0.344	0.044	0.086	0.240
Cl^-	0.005	0.000	0.000	0.003	0.000	0.000	0.000	0.000	0.000	0.000	0.000
OH^-	1.578	1.877	1.867	1.842	1.821	1.795	1.682	1.656	1.956	1.914	1.760
O^{2-}	11.578	11.877	11.867	11.842	11.821	11.795	11.682	11.656	11.956	11.914	11.760
catsum	7.750	7.790	7.803	7.758	7.760	7.793	7.775	7.775	7.736	7.798	7.762
ansum	12.000	12.000	12.000	12.000	12.000	12.000	12.000	12.000	12.000	12.000	12.000
Mg/(Mg+Fe)	0.246	0.399	0.455	0.307	0.436	0.404	0.292	0.385	0.383	0.446	0.326

(Tab. 4). Variable, but usually elevated, F contents (0.10–1.69 wt. %, 0.02–0.42 apfu) are common.

Garnet in tourmalinites forms equant grains up to 2 cm in diameter, typically of euhedral shape, but anhedral grains also occur. The crystals are often poikilitic (Fig. 2g), sometimes with extremely inclusion-rich cores. Quartz, tourmaline, muscovite, biotite and plagioclase are common minerals forming inclusions. The outer parts of the garnet grains are poor in inclusions. Garnet in the mica schists forms predominantly euhedral to subhedral rotated porphyroblasts up to 1 cm in diameter. It is typically poor in inclusions, or contains abundant inclusions of quartz (Fig. 5d). On the other hand, inclusions of garnet were commonly observed in tourmaline crystals (Fig. 5b).

Garnet represents an almandine-rich composition corresponding to $Alm_{79–92}$ $Prp_{4–15}$ $Sps_{0–13}$ $Grs_{0–4}$ $Adr_{0–3}$ in tourmalinites and $Alm_{64–88}$ $Prp_{3–15}$ $Sps_{1–20}$ $Grs_{0–19}$ $Adr_{0–3}$ in mica schists (Tab. 5). The central part (poikilitic in tourmalinites) of the garnet grains is chemically homogeneous or exhibits an increase in Fe and Mn and decrease in Mg and X_{Mg} toward the centre (Fig. 7a, c). Calcium contents are variable but are often the highest in the core. The outer zone of garnet grains is characterized by the rimward depletion in Mg and the enrichment in Mn and Fe (Fig. 7b, d).

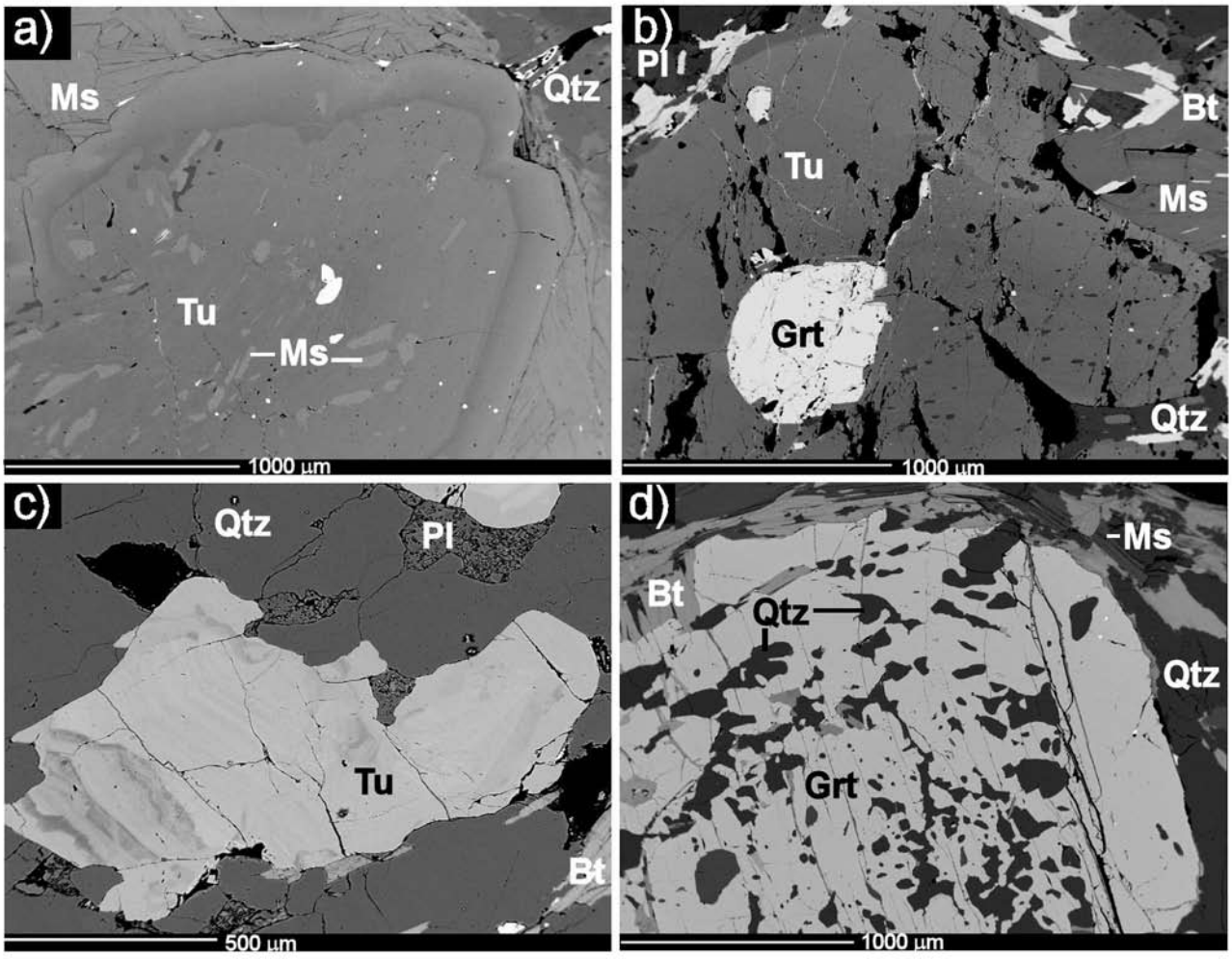

Fig. 5 Mica schists in BSE images. **a** – Tourmaline enclosing muscovite, Kozlov; **b –** Tourmaline enclosing garnet, Tišnov; **c** – Oscillatory zoned tourmaline grains, Kozlov; **d** – Garnet enclosing abundant quartz inclusions, Pernštejn. The symbols for rock-forming minerals used after Kretz (1983).

5.3. Whole-rock chemical composition of tourmalinites

The tourmalinites and the surrounding mica schists have mutually very similar chemical compositions (Tab. 6). This comparison is based on the complete chemical analyses including trace elements of 6 samples of tourmalinites and 4 samples of mica schists. The unpublished chemical analyses of tourmalinites (the major elements together with B and F determinations) of M. Novák were also included.

The SiO_2 and Al_2O_3 contents in the tourmalinites vary significantly, in accord to modal amounts of quartz and tourmaline. The tourmalinites compared to the chemical composition of the surrounding mica schists (Fig. 8a), are poorer in Na_2O (0.03–2.19 wt. %), K_2O (0.00–2.32 wt. %), Ba (16–280 ppm), Sr (13–110 ppm), Rb (11–75 ppm), Cs (0.2–2.8 ppm), and U (1.9–4.9 ppm). On the other hand, the tourmalinites exhibit relatively higher contents of MgO (1.1–4.6 wt. %) and high B (0.54–3.05 wt. %) with F (0.12–0.96 wt. %). The content of B in the mica schists varies significantly (13–3200 ppm) at relatively uniform but high F content (0.09–0.37 wt. %). Trace elements (Ba, Sr, Co, Cr, Ni, V, Cu, Zn, Sn, As) in tourmalinites are usually low, however, some samples are enriched in P (up 1.0 wt. % P_2O_5), As (up 170 ppm) or Sn (up 38 ppm).

The total REE contents range from 54 to 526 ppm. The chondrite-normalized REE patterns for tourmalinites and mica schists are fairly similar (Fig. 8b) with variable but usually distinct fractionation of the LREE (Ce_N/Sm_N = 1.3–3.3). The HREE show relatively flat trends (Gd_N/Yb_N = 0.7–2.8). A negative europium anomaly (Eu/Eu* = 0.4–0.6) is also characteristic.

Tab. 5 Representative chemical compositions of garnets from tourmalinites and mica schists

	Kovářová			Tišnov						Kozlov		
	tourmalinites						mica schists					
	rim	middle	core	rim	middle	core	rim	middle	core	rim	middle	core
P_2O_5	0.06	0.05	0.20	0.04	0.00	0.00	0.00	0.00	0.00	0.20	0.11	0.08
SiO_2	36.79	36.79	36.67	36.26	36.60	36.60	36.62	36.74	36.35	35.91	36.23	36.75
TiO_2	0.00	0.00	0.00	0.00	0.00	0.00	0.02	0.04	0.05	0.03	0.07	0.00
Al_2O_3	20.83	20.98	20.79	20.31	20.73	20.30	20.40	20.55	20.36	20.50	20.54	20.80
Cr_2O_3	0.00	0.00	0.00	0.00	0.00	0.00	0.02	0.02	0.00	0.02	0.03	0.00
Y_2O_3	0.00	0.00	0.00	0.00	0.00	0.00	0.00	0.06	0.00	0.00	0.00	0.00
Fe_2O_3*	0.00	0.04	0.42	0.64	0.79	1.19	0.38	0.77	0.94	1.60	1.17	1.26
FeO*	38.11	37.33	38.21	37.07	36.76	36.32	35.09	35.23	33.78	34.81	36.58	36.01
MnO	0.29	0.22	0.43	3.06	2.14	2.07	4.21	2.62	2.99	6.07	2.92	1.42
MgO	2.30	2.93	2.51	1.56	2.49	2.64	1.11	1.44	1.29	1.24	1.86	3.06
CaO	0.91	1.03	0.74	0.48	0.67	0.75	1.71	2.88	3.69	0.65	0.87	1.39
Na_2O	0.00	0.04	0.07	0.00	0.00	0.00	0.00	0.00	0.00	0.05	0.07	0.00
K_2O	0.00	0.00	0.00	0.00	0.00	0.00	0.03	0.00	0.00	0.00	0.00	0.00
Total	99.29	99.41	100.03	99.43	100.18	99.87	99.59	100.36	99.46	101.07	100.43	100.76
* Calculated on the basis of ideal stoichiometry and charge-balance calculation												
A-site												
Na^+	0.000	0.006	0.011	0.000	0.000	0.000	0.000	0.000	0.000	0.008	0.011	0.000
K^+	0.000	0.000	0.000	0.000	0.000	0.000	0.003	0.000	0.000	0.000	0.000	0.000
Ca^+	0.079	0.090	0.064	0.043	0.058	0.065	0.151	0.250	0.324	0.057	0.075	0.119
Mg^{2+}	0.281	0.355	0.303	0.191	0.301	0.320	0.136	0.175	0.158	0.150	0.225	0.366
Mn^{2+}	0.020	0.015	0.030	0.213	0.147	0.143	0.293	0.180	0.207	0.418	0.201	0.096
Fe^{2+}	2.604	2.535	2.592	2.553	2.494	2.472	2.410	2.392	2.312	2.368	2.488	2.418
Y^{3+}	0.000	0.000	0.000	0.000	0.000	0.000	0.000	0.003	0.000	0.000	0.000	0.000
subtotal	2.984	3.000	2.999	3.000	3.000	3.000	2.992	3.000	3.000	3.000	3.000	3.000
B-site												
Al^{3+}	2.002	1.998	1.974	1.960	1.952	1.927	1.974	1.949	1.938	1.899	1.923	1.924
Fe^{3+}	0.000	0.002	0.026	0.040	0.048	0.073	0.024	0.047	0.058	0.098	0.072	0.076
Cr^{3+}	0.000	0.000	0.000	0.000	0.000	0.000	0.001	0.001	0.000	0.001	0.002	0.000
Ti^{4+}	0.000	0.000	0.000	0.000	0.000	0.000	0.001	0.002	0.003	0.002	0.004	0.000
subtotal	2.002	2.000	2.000	2.000	2.000	2.000	2.000	2.000	2.000	2.000	2.000	2.000
T-site												
P^{5+}	0.004	0.003	0.013	0.003	0.000	0.000	0.000	0.000	0.000	0.014	0.008	0.005
Si^{4+}	3.006	2.987	2.974	2.986	2.970	2.979	3.008	2.983	2.975	2.920	2.946	2.950
Al^{3+}	0.004	0.010	0.013	0.011	0.030	0.021	0.000	0.017	0.025	0.066	0.046	0.044
subtotal	3.014	3.000	3.001	3.000	3.000	3.000	3.008	3.000	3.000	3.000	3.000	3.000
O^{2-}	12.015	11.994	11.996	11.996	11.985	11.990	12.007	11.994	11.989	11.971	11.977	11.980
Mg/(Mg+Fe)	0.097	0.123	0.105	0.070	0.108	0.115	0.054	0.068	0.064	0.060	0.083	0.132
mol. %												
pyrope	9.40	11.84	10.15	6.34	9.99	10.51	4.56	5.82	5.25	4.86	7.42	12.21
almandine	87.25	84.66	86.72	84.61	82.73	81.21	80.61	79.73	77.06	76.70	82.12	80.61
spessartine	0.68	0.50	0.99	7.07	4.87	4.68	9.79	6.01	6.90	13.54	6.63	3.21
grosulare	2.66	2.89	0.85	0.00	0.00	0.00	3.74	5.79	7.71	0.00	0.00	0.17
andradite	0.00	0.11	1.29	1.98	2.41	3.60	1.19	2.36	2.91	4.75	3.54	3.81
uvarovite	0.00	0.00	0.00	0.00	0.00	0.00	0.07	0.07	0.00	0.07	0.08	0.00
Mg/(Fe+Mg)	0.097	0.123	0.105	0.070	0.108	0.115	0.054	0.068	0.064	0.060	0.083	0.132

5.4. P-T metamorphic conditions

Thermobarometric conditions (P-T) of mica schists from the central and southern part of the SU were obtained using the garnet rims and matrix phases (muscovite, biotite, sillimanite and plagioclase). The calculated P-T conditions for this mineral assemblage yielded comparable results: the central part of the SU (Borovnice) – 598 ± 27 °C and 5.7 ± 1.2 kbar, the southern part of the SU – (Pernštejn) 625 ± 43 °C and 5.3 ± 1.8 kbar. Mica schists from Tišnov indicate P-T conditions of 642 ± 89 °C and 8.8 ± 3.4 kbar for the garnet rim and micas with plagioclase in the matrix.

6. Discussion

6.1. Tourmaline evolution

Unlike garnet, tourmaline in the tourmalinites commonly exhibits complex zoning. Comparable chemical compositions, zoning and substitution mechanisms in tourmalines from all the studied samples testify to the same origin of tourmalinites in the whole region. The tourmaline represents the oldest mineral in association, as no inclusions of other rock-forming minerals (except quartz) were found. On the other hand, the schorl cores (zone I), rimmed by narrow tourmaline of zone II with dominant dravite component are typically enclosed by garnet, annite, muscovite or kyanite (Fig. 2g–h). These relations suggest that the tourmaline of zone I and, in part, that of zone II, was produced before crystallization of the garnet and remaining phases.

The Al-rich schorl with a high X-site vacancy and relatively low fluorine content (zone I), is the oldest tourmaline generation in the tourmalinites of the SU. The presence of cores with a complex structure in the tourmaline crystals indicates multiphase evolution of the rocks. Chemical composition of tourmaline of the zone I is similar to that from quartz–tourmaline rocks for instance, at Mt. Isa, Broken Hill, Sundown Group (Australia) and in the Belt–Purcell Supergroup (Canada), where the tourmaline precipitated from Fe-rich exhalative fluids, which passed though a thick column of clay-rich sediments (Plimer 1983, 1988; Beaty et al. 1988; Slack 1993, 1996). The low fluorine content is probably crystallochemically controlled, with limited entry of F in tourmaline with a high X-site vacancy (Henry and Dutrow 1996). Our observations do not indicate that the tourmaline cores could represent grains of a pre-metamorphic

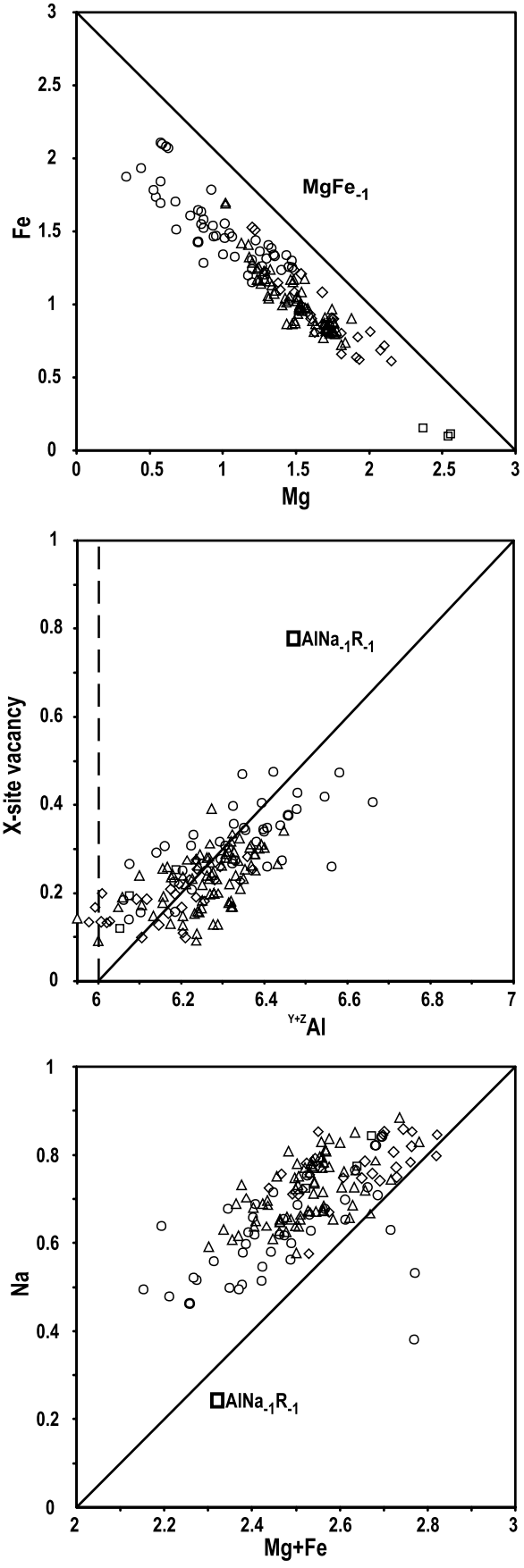

⇨

Fig. 6 Simple binary plots for tourmaline compositions used for testing of substitution mechanisms. Values are given in apfu.

Tab. 6 Representative whole-rock chemical compositions of tourmalinites and mica schists

rock type		tourmalinite			mica shist				tourmalinite			mica shist	
locality		Pernštejn	Kovářová	Nedvědice-S	Tišnov	Kozlov			Pernštejn	Kovářová	Nedvědice-S	Tišnov	Kozlov
SiO_2	wt. %	82.76	72.56	69.82	63.41	60.46							
TiO_2	wt. %	0.63	0.43	0.76	0.75	0.88	Ba	ppm	16.1	220	47.2	507	575
Al_2O_3	wt. %	9.84	14.93	16.69	19.26	20.81	Co	ppm	0.7	17.9	3.3	10.6	15.8
Cr_2O_3	wt. %	0.01	0.01	0.01	0.01	0.01	Cu	ppm	0.5	10.2	0.9	17.3	20.7
Fe_2O_3 tot	wt. %	2.53	3.98	6.87	5.19	6.68	Ni	ppm	2.5	19.0	5.8	27.4	14.4
MnO	wt. %	0.02	0.04	0.03	0.08	0.13	Rb	ppm	10.9	74.7	45.1	207	301
MgO	wt. %	1.32	2.07	2.42	1.39	1.85	Sr	ppm	13.4	36.8	56.1	108	78.1
CaO	wt. %	0.09	0.62	0.15	0.44	0.39	V	ppm	45.0	79.0	81.0	95.0	118
Na_2O	wt. %	0.47	0.73	0.75	1.92	0.87	Sn	ppm	10.0	7.0	38.0	12.0	12.0
K_2O	wt. %	0.21	1.70	0.61	3.82	4.65	Zn	ppm	<1	7.0	5.0	31.0	50.0
P_2O_5	wt. %	0.04	0.39	0.07	0.13	0.11	As	ppm	1.1	170	3.0	3.1	110
LOI	wt. %	1.30	2.40	1.80	3.40	3.10	U	ppm	3.1	3.4	4.9	6.8	6.2
Total	wt. %	99.22	99.87	99.99	99.81	99.95	Nb	ppm	12.9	7.6	15.8	17.2	18.4
Mg/(Mg+Fe)		0.31	0.31	0.23	0.19	0.19	Mo	ppm	0.1	0.2	0.1	0.2	0.5
							Y	ppm	32.6	51.2	41.0	31.6	36.2
La	ppm	46.5	24.8	110	44.0	52.7	Zr	ppm	780	71.6	246	166	161
Ce	ppm	105	51.7	229	87.8	104	Pb	ppm	0.6	1.1	0.8	2.3	4.6
Pr	ppm	11.6	6.6	28.1	10.6	12.9	Cd	ppm	<0.1	0.1	0.1	0.1	0.2
Nd	ppm	43.3	27.3	105	38.9	49.3	Cs	ppm	0.2	2.8	2.7	6.9	15.1
Sm	ppm	7.7	6.2	19.1	7.3	8.8	Th	ppm	19.6	10.5	17.7	16.8	19.1
Eu	ppm	1.2	1.1	2.3	1.3	1.7	Ta	ppm	<0.1	2.1	1.2	3.0	1.4
Gd	ppm	6.0	7.6	12.2	5.7	6.9	Hf	ppm	21.2	2.4	7.3	5.4	5.0
Tb	ppm	1.0	1.6	1.9	1.0	1.2	Sc	ppm	5.0	14.0	10.0	15.0	17.0
Dy	ppm	5.2	8.8	8.6	5.3	6.6	Au	ppb	<0.5	3.9	0.7	1.3	0.5
Ho	ppm	1.1	1.8	1.4	1.1	1.2	Sb	ppm	<0.1	0.1	<0.1	0.1	0.3
Er	ppm	3.4	4.9	3.9	3.1	3.6	Ag	ppm	<0.1	<0.1	<0.1	<0.1	<0.1
Tm	ppm	0.5	0.7	0.6	0.5	0.6	Hg	ppm	<0.1	<0.1	0.0	<0.1	0.0
Yb	ppm	3.3	4.2	3.5	3.1	3.3	Tl	ppm	0.1	0.2	0.2	0.4	1.0
Lu	ppm	0.5	0.6	0.5	0.5	0.5	Bi	ppm	<0.1	6.2	0.2	0.6	0.2
							W	ppm	8.1	1.7	4.0	5.7	6.5
F	ppm	1780	1180	1640	1270	3560	Ga	ppm	14.0	23.0	19.9	25.1	27.9
B	ppm	7002	6947	11348	596	3198	Se	ppm	<0.5	<0.5	<0.5	<0.5	<0.5

detrital tourmaline, namely: i) continuous compositional trends for tourmalines in the individual zones, as well as at all the studied localities, ii) an accessory mineral assemblage. Regarding the latter point, high abundance of detrital tourmaline is typical of an ultra-stable association of heavy detrital minerals, characterized by the zircon and rutile presence. However, in the studied samples, zircon is rare, and rutile in the form of anhedral grains incorporated in the mosaics of silicate minerals is probably not of detrital origin.

Rarely, the schorl cores carry minute dravite domains (the Tišnov locality) indicating a complex, pre-metamorphic history. It is not possible to exclude a detrital origin in these cases and their primary origin is problematic. Magnesium-rich tourmaline is typical of metacarbonates (dolomites), metaevaporite sequences, ultramafic rocks, Cr- and V-rich metasediments or granulite-facies rocks. However, the Cr and V contents, which are typical of the tourmaline from ultramafic rocks and or Cr- and V-rich metasediments (Treloar 1987; King and Kerrich 1989; Michailidis et al. 1995), are in the inner dravite cores below the detection limit of the EMPA. Tourmaline from metacarbonates usually contains a high uvite component (Brown and Ayuso 1985; Henry and Guidotti 1985), but the Ca contents in the studied dravite core are very low (below 0.03 apfu Ca). A high-grade metamorphic origin is probable, although tourmaline is rarely found in granulite-facies rocks (Broken Hill, Australia; the Acadian granulite-facies region, the south–central Massachusetts), in which the second sillimanite isograd has been exceeded (Slack et al. 1993; Thomson 2006). However, high Ti contents typical of the tourmaline from high-temperature

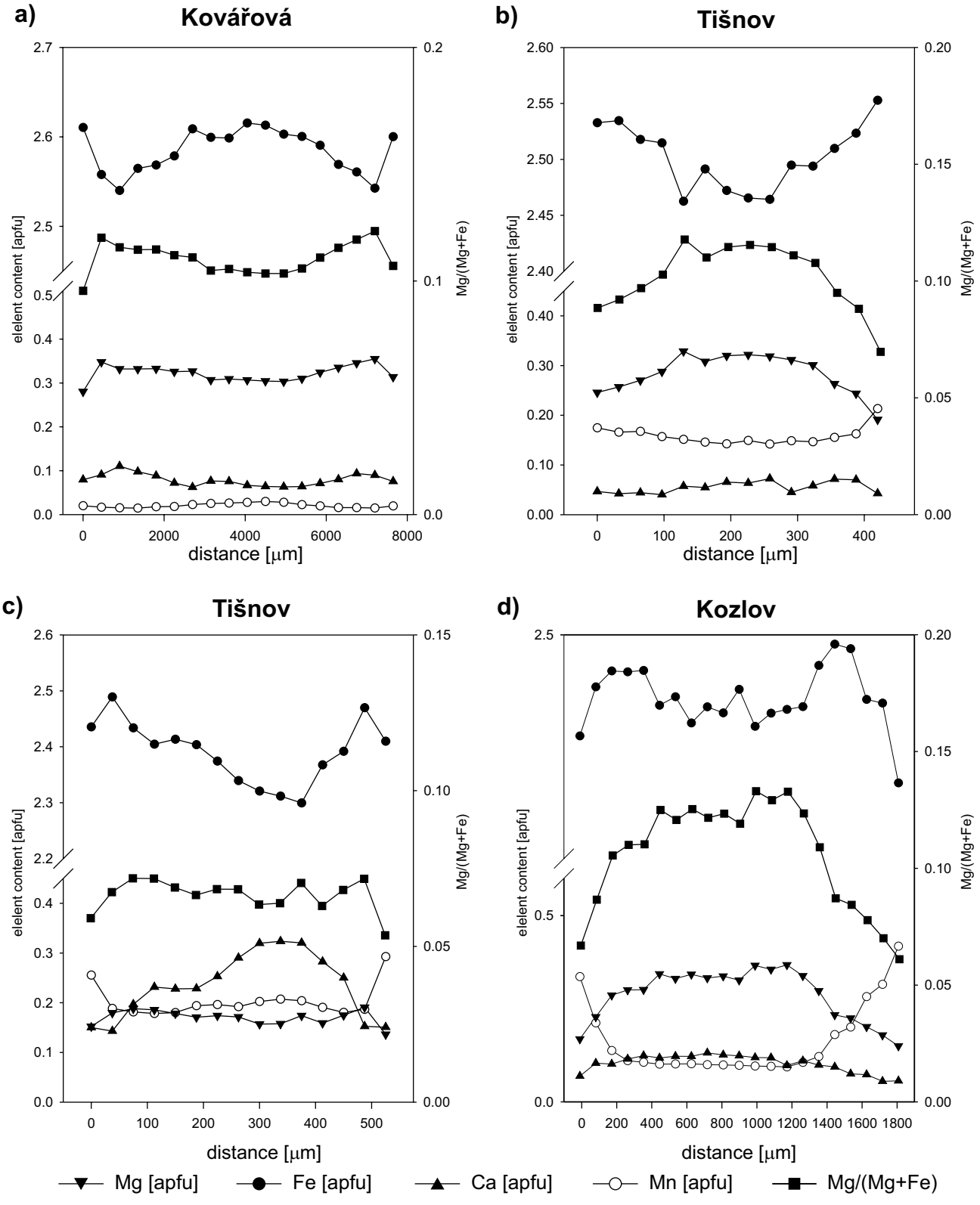

Fig. 7 Garnet zoning in selected samples of tourmalinites (a–b) and associated mica schists (c–d).

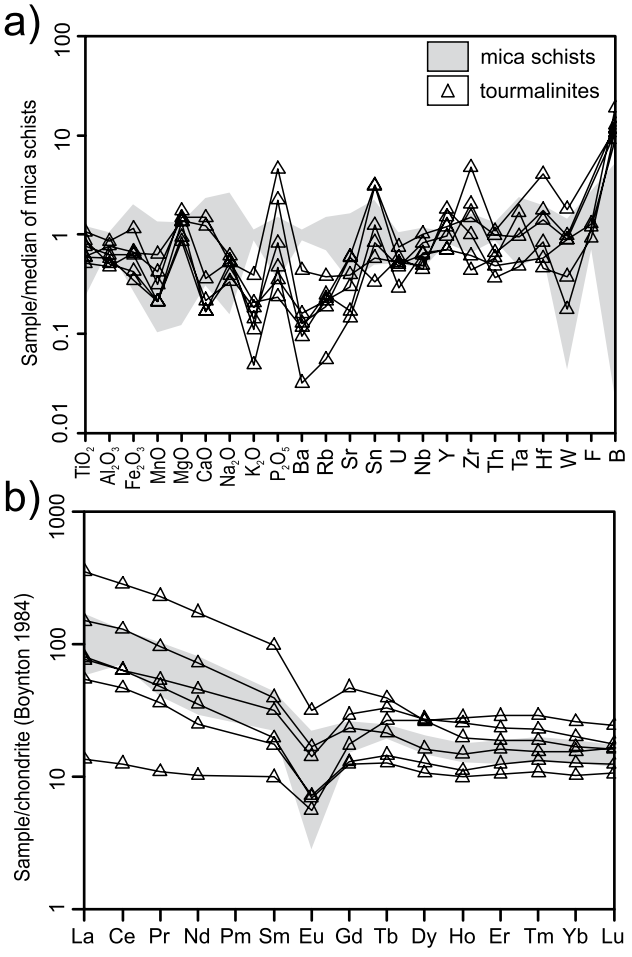

Fig. 8 Comparison of the chemical compositions of tourmalinites and mica schists. **a** – Selected oxides and elements normalized to the median composition of mica schists; **b** – Chondrite-normalized (Boynton 1984) REE patterns for tourmalinites and mica schists.

metamorphic rocks (Willner 1992) are missing in these inner dravite cores (< 0.2 wt. % TiO_2).

Based on chemical composition and textural relationship with other rock-forming minerals, dravite rich in F and Na, and having a low X-site vacancy (zone II) overgrowing or replacing the schorl core (zone I), probably corresponds to crystallization of tourmaline in the course of prograde metamorphism. Elevated P-T conditions stabilize increased F and Na in tourmaline, and a high X_{Mg} is characteristic of tourmaline crystallized in metapelites under amphibolite-facies conditions (Henry and Guidotti 1985; Grew et al. 1990; Henry and Dutrow 1996, 1997). Because of the tourmaline's wide stability range (Werding and Schreyer 1984), the primary composition of this mineral in tourmaline-rich rocks of many localities worldwide (e.g. Mt. Isa Orogen, Olary Block, Broken Hill Block; Australia) is preserved regardless a later metamorphic overprint even under amphibolite- and granulite-facies conditions (Taylor and Slack 1984; Plimer 1988). Additional input of F- and B-rich fluids is supposed for growth of this younger metamorphic tourmaline. It is probable that partial melting of gneisses in the SU took place during this stage of prograde metamorphism, resulting in crystallization of the associated peraluminous migmatites or metagranites, which also contain F-rich tourmaline (Němec 1979; Melka et al. 1992; Novák et al. 1998). The associated metagranites represented another potential source of B- and F-rich fluids.

Relatively homogeneous tourmaline with the schorl–dravite composition in the outer parts of the crystals (zone III), characterized by a slight decline in X_{Mg} and F toward the crystal margin, represents possibly a product of retrograde metamorphism, accompanied by introduction of B- and F-rich fluids. Calculated P-T conditions ~ 600–630 ºC and 5–6 kbar for the mica schists of the southern and central part of the SU are interpreted as being a product of retrograde metamorphism marked by disappearance of kyanite and staurolite as well as growth of garnet porphyroblasts associated with sillimanite (for more details see Buriánek and Čopjaková 2008). The tourmaline rims in the tourmalinites from Jimramov contain relatively high Ca (0.104–0.138 apfu). Garnet in these samples also has an increased Ca (0.12–0.17 apfu) compared to garnets in other tourmalinite samples. It is possible that Ca was derived from associated gneisses, in which Ca-rich cores of plagioclase were exposed in the process of deformation during the retrogression stage.

The chemical compositions of the tourmaline (zones II and III) from tourmalinites and those from the surrounding mica schists are rather similar. The central part of the tourmaline (dravite) from the mica schists corresponds to the zone II in the tourmaline from tourmalinites. Moreover, a predominant part of schorl–dravite from mica schists containing inclusions of garnet, biotite and muscovite is comparable with outer zone of the tourmaline (zone III) from tourmalinites. The chemical composition of tourmaline reflects its metamorphic grade. The dravite in the central part of tourmaline crystals from the mica schists exhibits the compositional characteristics of tourmaline crystallized during a prograde metamorphism at the amphibolite-facies conditions (Henry and Guidotti 1985; Henry and Dutrow 1996, 1997), characterised by the mineral assemblage Qtz + Ms + Bt + Tu ± Ky ± St ± Grt. The second generation of tourmaline (schorl–dravite) was formed during exhumation of the SU, simultaneously with decompression breakdown of staurolite, according to the reaction St + Ms + Qtz = Grt + Sill + Bt + H_2O (Buriánek and Čopjaková 2008). As a result of this reaction, muscovite breakdown could release some B and F for tourmaline formation.

Tourmaline in the tourmalinites as well as in the country-rock mica schists represents the mineral richest

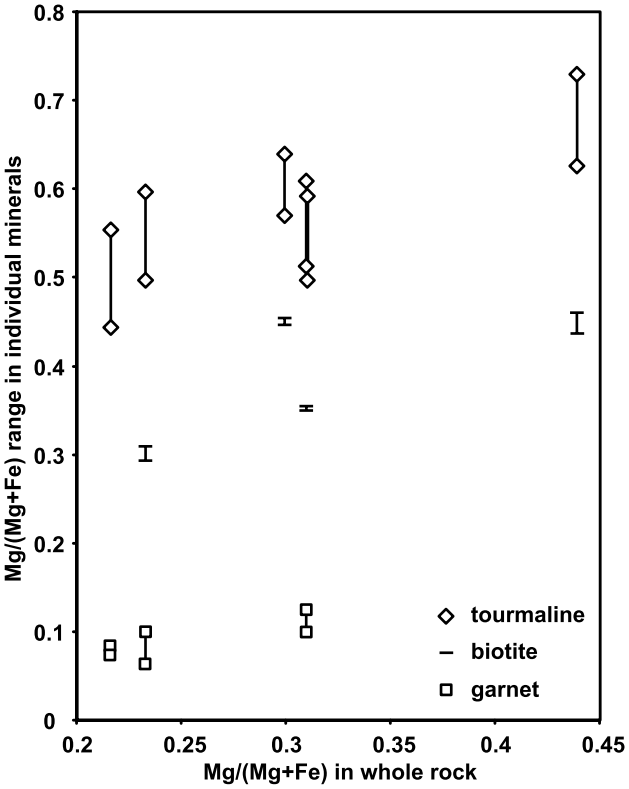

Fig. 9 Positive correlation of Mg/(Mg + Fe) in tourmaline, biotite and garnet (molar ratio) from tourmalinites and Mg/(Mg + Fe) of their whole-rock analyses (ratio in wt. %). The range of Mg/(Mg + Fe) in individual minerals for each sample is also shown.

in Mg. In all the tourmalinite samples, where tourmaline coexists with biotite ± garnet, the tourmaline exhibits a higher average X_{Mg} (except for older pre-Variscan schorl cores) than biotite and garnet according to the scheme Grt < Bt < Tu (compare Tabs 2, 4–5 and Fig. 9) . The values of X_{Mg} for the main rock-forming minerals from all the samples of mica schists increase in the order Grt < St < Bt < Tu (Buriánek and Čopjaková 2008). The X_{Mg} values of the whole-rock samples show a positive correlation with the X_{Mg} of individual ferromagnesian minerals (tourmaline, biotite, garnet and staurolite). The positive correlation in tourmalinites mentioned above is illustrated in Fig. 9. The differences in X_{Mg} of tourmaline and associated minerals at individual localities reflect Mg/(Mg + Fe) ratio in the rock.

In this sense, tourmaline provides valuable information regarding the evolution of tourmalinites and the associated rocks.

6.2. Compositional evolution of garnet

The majority of the examined garnet grains exhibit a flat diffuse compositional zoning in the core, which is characteristic of rocks in the upper parts of the amphibolite-facies conditions. The central (poikilitic) part of large garnet porphyroblasts in the tourmalinites represents growth during a prograde metamorphism with typical prograde zoning manifested by an increase in Mg and decrease in Fe (and sometimes also Mn) from the centre outwards. The simultaneous growth of the tourmaline of zone II with garnet is evident from textural relations. Observed prograde metamorphic zoning in garnet cores indicates that the tourmaline zone II grew during this metamorphic event. A similar prograde metamorphic zoning was, albeit rarely, observed also in the cores of garnet grains from the mica schists (Fig. 7a, c). The peak P-T conditions of this prograde metamorphism could not be determined because of the absence of suitable inclusions in the garnet. The chemical zoning in marginal part of garnets (a rimward decrease in Mg, Ca and an increase in Mn and Fe) in both tourmalinites and mica schists testifies to garnet growth during decreasing pressure and temperature (Spear et al. 1995) (Fig. 7b, d). The second garnet generation in mica schists probably resulted from the staurolite-consuming reaction St + Ms + Qtz = Grt + Sill + Bt + H_2O. Textural relations of garnet and tourmaline in mica schists support tourmaline formation predominantly (excluding dravite cores) during retrograde phase of metamorphism.

6.3. Whole-rock chemistry and origin of tourmalinites and associated mica schists

The tourmalinites at all the localities have a similar chemical composition and an analogous geological setting. Major element chemical composition of tourmalinites resembles many tourmalinites worldwide and reflects the variation in the modal content of the rock-forming minerals (Plimer 1986, 1987, 1988). Differences in the chemical compositions between mica schists and tourmalinites correlate well with differences in the mineralogical compositions of the two rock groups. The considerable similarity in the chemistry of tourmalinites and mica schists, including the REE patterns, suggests a similar protolith for the both rock types. The variation in most of elements reflects the variation in the mineralogical composition, associated with the transition from mica schist to tourmalinite. The decline in Ca, Na, K, Ba and Sr abundances is correlated with decreasing quantities of micas and feldspars, whereas the increase in Mg and B in the tourmalinites corresponds to the increase in the tourmaline content. Similar whole-rock geochemical trends were observed in tourmalinites and associated metapelites in other regions (Slack 1993; Shaw et al. 1993).

The increased content of the paragonite component in muscovite probably reflects the chemical composition of

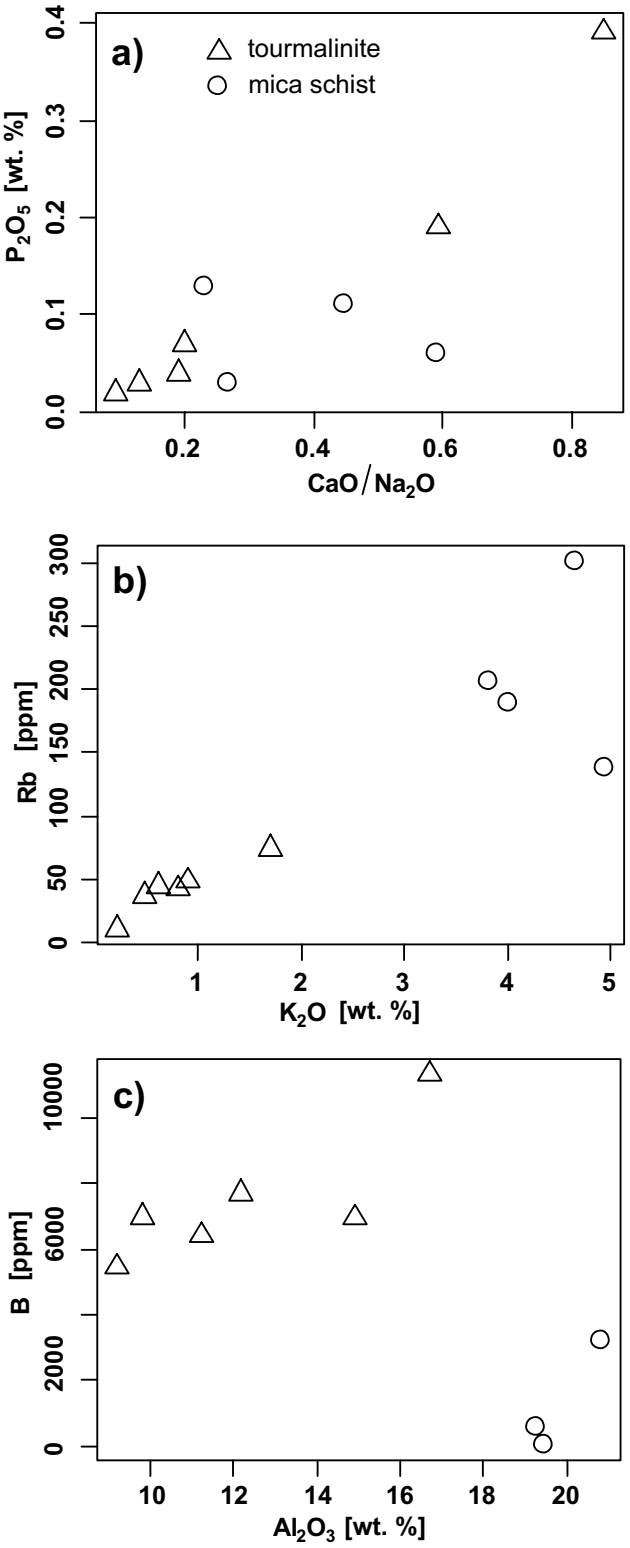

Fig. 10 Relations in whole-rock chemical compositions of tourmalinites and mica schists expressed as binary plots of selected components.

tourmalinites. As micas represent minerals crystallized or re-equilibrated during the retrograde metamorphism, it is unlikely that the elevated contents of the paragonite component indicate elevated pressure during metamorphism.

The CaO/Na_2O vs. P_2O_5 binary diagram (see Fig. 10a) shows a positive correlation between CaO and P_2O_5 in the tourmalinites. However, a positive correlation between Na_2O and CaO was observed in mica schists. These relationships indicate apatite as the main carrier of CaO in tourmalinites. However, in mica schists the content of CaO depends mainly on the quantity of plagioclase and its composition. The positive correlations in plots K_2O vs. Rb and Al_2O_3 vs. B in tourmalinites (see Fig. 10b–c) are in good agreement with a low content of feldspars and a high content of tourmaline.

The high, though rather variable, contents of F and B in the tourmalinites show a good mutual correlation and reflect the quantity of tourmaline in the rock. In the mica schists, a high F content reflects a high proportion of fluorine-bearing micas, but the variable boron content (13–3198 ppm B) always depends on the presence of tourmaline.

The fluorine contents in the southern and central parts of the SU (0.12–0.96 wt. % in tourmalinites; 0.09–0.37 wt. % in mica schists) are higher than in ordinary metapelites abroad. For instance, Torres-Ruiz et al. (2003) reported contents of 0.13–0.15 wt. % F for tourmalinites and 0.07–0.13 wt. % F for country-rock metapelites. The increased fluorine contents are characteristic for tourmaline, biotite and muscovite, both in tourmalinites (Tu ≤ 0.51 apfu; Ms ≤ 0.27 apfu; Bt ≤ 0.42 apfu), and in the country-rock mica schists (Tu ≤ 0.39 apfu; Ms ≤ 0.51 apfu; Bt ≤ 0.36 apfu). The two-mica schists with garnet and staurolite, typical of the northern part of the SU, contain lower fluorine abundances in the individual minerals. However, they still remain relatively high (tourmaline up to 0.2 apfu; muscovite up to 0.34 apfu; biotite up to 0.35 apfu) (Buriánek and Čopjaková 2008).

Locally increased contents of P (up to 1.0 wt. % P_2O_5), As (up to 170 ppm) and Sn (up to 38 ppm) can support the hydrothermal origin of tourmalinites. As noted by Kebrt et al. (1984), it is more probable that protolith of tourmalinites and their country-rock metapelites represented sedimentary rocks with primary enrichment in B, and possibly also F and Fe (exhalites). In their view, the tourmalinites could have been formed by reaction of relatively low-temperature hydrotherms with pelites in the original sedimentary basin. The elevated contents any of other elements Pb, Zn, Cu, Co, Cr, Ba or Sr might indicate submarine exhalative origin of hydrothermal fluids (Taylor and Slack 1984; Plimer 1987). However, the concentrations of these elements are typically low in studied rocks.

In a lithostratigraphic context, the tourmalinite occurrences are limited to a level above the Nedvědice marbles.

Some rocks (especially migmatites and metagranites) of the surrounding metamorphic complex are anomalously rich in Sn, As, F, Bi, and B (Němec 1979, 1980). Enrichment in these elements is typical of infiltration iron-rich skarns enclosed inside Nedvědice marbles (Houzar and Hrazdil 2009). Input of P, As and Sn by hydrothermal granitic fluids from associated metagranites cannot be excluded. Direct derivation of all F- and B-rich fluids from neighbouring metagranite and migmatite bodies is unlikely with regard to the absence of clear field relations among tourmalinites, migmatites and metagranites. This lack of field association was already noted by Němec (1979, 1980).

7. Conclusions

Tourmalinites (rocks with an association Tu + Qtz + Ms ± Grt ± Bt ± Ky ± Sil ± Pl ± Kfs) from the Svratka Unit form stratiform layers hosted in mica schists with mineral association Qtz + Ms + Bt + Tu ± Ky ± Grt. Similarities in the chemical composition of the tourmalinites and the mica schists suggest a similar protolith to the both rock types. Tourmalinites are interpreted as a part of a metamorphosed volcano-sedimentary complex primarily rich in F and B. However, the derivation of all the F- and B-rich fluids from the neighbouring migmatites and metagranites is unlikely.

The chemical composition of tourmaline from both tourmalinites and mica schists varies from Al-rich schorl to dravite. The compositional variability of tourmaline is controlled predominantly by the $(^{X}\square\,^{Y}Al\,^{W}OH)$ $(^{X}Na\,^{Y}Mg\,^{W}F)_{-1}$ and $^{Y}Fe^{Y}Mg_{-1}$ substitutions.

The presence of brecciated tourmaline cores with a complex structure in tourmalinites indicates multiphase evolution of the rocks. These cores (Al-rich schorl with a high X-site vacancy) are interpreted as an older, low-temperature hydrothermal (probably volcano exhalative fluids) tourmaline.

The next generation of tourmaline (dravite composition) in tourmalinites as well as tourmaline cores from mica schists exhibits compositional characteristics of the prograde, amphibolite-facies metamorphic event characterised in mica schists by the mineral assemblage Qtz + Ms + Bt + Tu ± Ky ± St ± Grt.

The last generation of tourmaline (schorl–dravite) present in both the mica schists and tourmalinites, formed during exhumation of the Svratka Unit accompanied by decreasing pressure and temperature. In the mica schists, this event resulted in decompression breakdown of staurolite, according to the reaction St + Ms + Qtz = Grt + Sil + Bt + H_2O. The P-T conditions of this retrograde metamorphism were calculated at 600–640 °C and 5–6 kbar.

Acknowledgements Financial support from the Ministry of Environment of the Czech Republic (project No. 6352) and the Czech Geological Survey internal project No. 3270 are gratefully acknowledged. The authors are grateful to S. Vrána and M. Štulíková for English corrections as well as P. Uher and A. Pieczka for critically reviewing this contribution.

Electronic supplementary material. The GPS coordinates of the studied samples (Tab. 1), and the tables of representative chemical analyses of tourmaline, biotite, muscovite, garnet and whole-rock chemical data (Tabs 2–6) are available online at the Journal web site *(http://dx.doi.org/10.3190/jgeosci.048)*.

References

Abraham K, Mielke H, Povondra P (1972) On the enrichment of tourmaline in metamorphic sediments of the Arzberg Series, W. Germany (NE Bavaria). Neu Jb Mineral, Mh 5: 209–219

Appel PWU (1985) Strata-bound tourmaline in the Archean Malene supracrustal, West Greenland. Canad J Earth Sci 22: 1485–1491

Beaty DW, Hahn GA, Threlkeld WE (1988) Field, isotopic, and chemical studies of tourmaline-bearing rocks in the Belt–Purcell Supergroup: genetic constraints and exploration significance for Sullivan type ore deposits. Canad J Earth Sci 25: 392–402

Blažková Š (2005) Metamorphic and structural evolution of the skarn near Věcnov. Unpublished MSci. Thesis, Masaryk University, Brno, pp 1–37 (in Czech)

Boynton, WR (1984) Cosmochemistry of the rare earth elements meteorite studies. In: Henderson, P (ed) Rare Earth Element Geochemistry. Elsevier, Amsterdam, pp 63–114

Brown CE, Ayuso RA (1985) Significance of tourmaline-rich rocks in the Grenville Complex of St. Lawrence County, New York. U S Geol Surv Bull 1626-C, pp 1–33

Buriánek D, Čopjaková R (2008) Tourmaline from the mica schist of the Svratka Crystalline Complex. Acta Mus Moraviae, Sci Geol 93: 61–80 (in Czech)

Buriánek D, Čech S, Vít J (2006) Basic geological map ČR 1 : 25 000, 24-112 Jedlová. Czech Geological Survey. Prague (in Czech)

Buriánek D, Břízová E, Čech S, Čurda J, Fürych V, Hanžl P, Kirchner K, Lysenko V, Roštínský P, Rýda K, Skácelová D, Skácelová Z, Vít J, Verner K (2009) Basic geological map ČR 1:25 000 with explanations, sheet 24-112 Jedlová. Czech Geological Survey. Prague, pp 1–76 (in Czech)

Chown EH (1987) Tourmalinites in the Aphebian Mistassini Group, Quebec. Can J Earth Sci 24: 826–830

Čopjaková R, Buriánek D, Škoda R, Houzar S (2007) Tourmalinites from the southern part of the Svratka Crystalline Complex. Acta Mus Moraviae, Sci Geol 92: 111–130 (in Czech)

Grew ES, Chernosky JV, Werding G, Abraham K, Marquez N, Hinthorne NJ (1990) Chemistry of kornerupine and associated minerals, a wet chemical, ion microprobe, and X-ray study emphasizing Li, Be, B and F contents. J Petrol 31: 1025–1070

Hanžl P, Vít J (2005) Basic geological map ČR 1 : 25 000, 14-333 Svratka. Czech Geological Survey, Prague (in Czech)

Hanžl P, Hrdličková K, Vít J (2006) Basic geological map ČR 1 : 25 000, 24-132 Dalečín. Czech Geological Survey, Prague (in Czech)

Hawthorne FJ, Henry DJ (1999) Classification of the minerals of the tourmaline group. Eur J Mineral 11: 201–216

Henry DJ, Dutrow BL (1996) Metamorphic tourmaline and its petrologic applications. In: Grew E, Anovitz L (eds) Boron: Mineralogy, Petrology, and Geochemistry in the Earth's Crust. Mineralogical Society of America Reviews in Mineralogy 33: 503–557

Henry DJ, Dutrow BL (1997) Tourmaline in sedimentary and metamorphic rocks. In: Novák M, Selway JB (eds) Tourmaline 1997, Abstract volume. Moravian Museum, Brno, pp 36–37

Henry D, Guidotti VCh (1985) Tourmaline as a petrogenetic indicator mineral: an example from the staurolite-grade metapelites of NW Maine. Amer Miner 70: 1–15

Holland TJB, Powell R (1998) An internally consistent thermodynamic data set for phases of petrological interest. J Metamorph Geol 16: 309–343

Houzar S, Hrazdil V (2009) Nordenskioldine $CaSnB_2O_6$ from the locality Kozlov near Nedvědice, new rare accessoric mineral for Nedvědice marbles. Acta Mus Moraviae, Sci Geol 94: in print (in Czech)

Houzar S, Novák M (2006) Occurrence of the Nedvědice type marbles at Klucanina near Tišnov. Geol výzk Mor Slez v r 2005 13: 86–88 (in Czech)

Houzar S, Novák M, Selway JB (1997) Pernštejn near Nedvědice: metamorphosed tourmalinites in mica schists. Tourmaline minerals: dravite, schorl. Novák M, Selway JB (eds) Tourmaline 1997, Field Trip Guidebook. Moravian Museum, Brno, pp 71–83

Houzar S, Novák M, Selway JB (1998) Compositional variation in tourmaline from tourmalinite and quartz segregations at Pernštejn near Nedvědice (Svratka Unit, western Moravia, Czech Republic). J Czech Geol Soc 43: 53–58

Houzar S, Doležalová H, Novák M, Hrazdil V, Pfeiferová A (2006) Mineralogy, petrography and geology of the Nedvědice marbles, Svratka crystalline complex; a review. Acta Mus Moraviae, Sci Geol 91: 3–77

Janoušek V, Farrow CM, Erban V (2006) Interpretation of whole-rock geochemical data in igneous geochemistry: introducing Geochemical Data Toolkit (GCDkit). J Petrol 47: 1255–1259

Kebrt M, Lhotský P, Pertold Z, Adam J (1984) Tourmalinites and tourmaline quartzites from Bohemian Massif. In: Correlation of Proterozoic, Paleozoic and Stratiform Deposits – Abstracts. Czech Geological Survey and Geological Institute of the Czech Academy of Sciences, Prague, pp 85–101

King RW, Kerrich R (1989) Chromian dravite associated with ultramafic-rock-hosted Archean lode gold deposits, Timmins–Porcupine district, Ontario. Canad Mineral 27: 419–426

Kretz R (1983) Symbols for rock-forming minerals. Amer Miner 68: 277–279

Lhotský P (1982) Tungsten mineralization at Deštné near Jindřichův Hradec. Unpublished MSci. Thesis, Faculty of Science, Charles University, Prague, pp 1–78 (in Czech)

Melichar R, Hanžl P, Vít J (2004) Basic geological map ČR 1:25 000, 24-111 Sněžné. Czech Geological Survey, Prague (in Czech)

Melka R, Schulmann K, Schulmannová B, Hrouda F, Lobkowicz M (1992) The evolution of perpendicular linear fabrics in synkinematically emplaced tourmaline granite (central Moravia–Bohemian Massif). J Struct Geol 14: 5, 605–620

Michailidis K, Sklavounos S, Plimer I (1995) Chromian dravite from the chromite ores of Vavdos area, Chalkidiki Peninsula, Northern Greece. Neu Jb Mineral, Mh 513–528

Mrázová Š, Otava J (2005) Basic geological map ČR 1 : 25 000 sheet 13-444 Hlinsko. Czech Geological Survey, Prague (in Czech)

Němec D (1979) Zinnbringende Orthogneise im Süden der Antiklinale von Svratka (nordwestlich Brno) und ihre Erzmineralisierung. Z Geol Wiss 12: 1437–1447

Němec D (1980) Fluorine phengites from tin-bearing orthogneisses of the Bohemian–Moravian Heights, Czechoslovakia. Neu Jb Mineral, Abh 139:155–169

Němec D (1986) Distinction of regionally metamorphosed greisens from metapelitic mica schists. Geol Rundsch 75: 685–692

Novák M, Selway JB, Houzar S (1998) Potassium-bearing, fluorine-rich tourmaline from metamorphosed fluorite layer in leucocratic orthogneiss at Nedvědice, Svratka Unit, western Moravia. J Czech Geol Soc 43: 37–44

Novotná B (1987) Petrostructural analysis of metamorphic rocks abroad skarn body near Věchnov. Unpublished MSci. Thesis, Faculty of Science, Charles University, Prague, pp 1–89 (in Czech)

Páša J, Hranáč P (1994) Tourmaline rocks. Unpublished Final report of the project Nr. 29 90 2301. Geomin, Jihlava pp 1–72 (in Czech)

Pertold Z, Chrt J, Budil V, Burda J, Burdová P, Kříbek B, Pertoldová J Gaskarth B (1994) The Tisová Cu-

deposit: a Besshi-type mineralization in the Krušné hory Mts., Bohemian Massif, Czech Republic. In: Monograph Series on Mineral Deposits 31: pp 71–95

Pertoldová J (1986) Conditions of origin of skarns on the deposits near Pernštejn, Županovice and Nové Město pod Smrkem. Unpublished PhD thesis, Faculty of Science, Charles University, Prague, pp 1–86 (in Czech)

Pertoldová J, Pertold Z, Pudilová M (1998) Metamorphic Development of Skarns at Pernštejn, Svratka Crystalline Complex, Bohemian Massif. J Czech Geol Soc 43: 191–202

Pertoldová J, Týcová P, Verner K, Košuličová M, Pertold Z, Košler J, Konopásek J, Pudilová M (2009) Metamorphic history of skarns, origin of their protolith and implications for genetic interpretation; an example from three units of the Bohemian Massif. J Geosci 54: 101–134

Plimer IR (1983) The association of tourmaline-bearing rocks with mineralisation at Broken Hill, NSW. In: Parkeville V (ed) The Australian I. M. M. Conference, Broken Hill NSW, pp 157–176

Plimer IR (1986) Tourmalinites from the Golden Dyke Dome, northern Australia. Miner Depos 21: 263–270

Plimer IR (1987) The association of tourmalinite with stratiform scheelite deposits. Miner Depos 22: 282–291

Plimer IR (1988) Tourmalinites associated with Australian Proterozoic submarine exhalative ores. In: Friedrich GH, Herzig PM (eds) Base Metal Sulphide Deposits. Springer–Verlag, Berlin, pp 255–283

Pouchou JL, Pichoir F (1985) „PAP" (Z) procedure for improved quantitative microanalysis. In: Armstrong JT (eds): Microbeam Anal. 1985. San Francisco Press, San Francisco, pp 104–106

Rambousek P (1983) Geologic prospecting of deposits near Žacléřská Bouda and Smrčí. Unpublished MSci. Thesis, Faculty of Sciences, Charles University, Prague, pp 1–135 (in Czech)

Shaw DR, Hodges CJ, Leitch CHB, Turner RJW (1993) Geochemistry of tourmalinite, muscovite, and chlorite-garnet-biotite alteration, Sullivan Zn-Pb deposit, British Columbia. Current Research, Part A; Geological Survey of Canada, Paper 93-1 A, 97–107

Slack JF (1993) Models for tourmalinite formation in the Middle Proterozoic Belt and Purcell supergroups (Rocky Mountains) and their exploration significance. Current Research, Part E; Geological Survey of Canada, Paper 93-lE, 33–40

Slack JF (1996) Tourmaline associations with hydrothermal ore deposits. In: Grew ES, Anovitz L M (eds) Boron: Mineralogy, Petrology and Geochemistry. Mineralogical Association of America Reviews in Mineralogy 33: 559–644

Slack JF, Herriman N, Barnes RG, Plimer IR (1984) Stratiform tourmalinites in metamorphic terranes and their geologic significance. Geology 12: 713– 716.

Slack JF, Palmer MR, Stevens BPJ, Barnes RG (1993) Origin and significance of tourmaline-rich rocks in the Broken Hill district, Australia. Econ Geol 88: 505–541

Spear FS, Kohn MJ, Paetzold S (1995) Petrology of the regional sillimanite zone, west-central New Hampshire, U.S.A. with implications for the development of inverted isograds. Amer Miner 80: 361–376

Šrein V, Šťastný M, Šreinová B, Langrová A (1997) Tourmaline from Měděnec (CZ) and Pöhla (D) Krušné Hory Mts. In: Novák M, Selway JB (eds) Tourmaline 1997, Abstract volume. Moravian Museum, Brno, pp 101–102

Tajčmanová L, Verner K, Pertoldová J (2005) Correlation of structural and metamorphic evolution of metamorphic rocks from the Svratka and Polička crystalline complexes. Geolines 19: 112

Taylor BE, Slack JF (1984) Tourmalinites from Appalachian–Caledonian massive sulfide deposits: textural, chemical, and isotopic relationships. Econ Geol 79: 1703–1726

Thomson JA (2006) A rare garnet–tourmaline–sillimanite–biotite–ilmenite–quartz assemblage from the granulite-facies region of south-central Massachusetts. Amer Miner 91: 1730–1738

Torres-Ruiz J, Pesquera A, Gil-Crespo PP, Velilla N (2003) Origin and petrogenetic implications of tourmaline-rich rocks in the Sierra Nevada (Betic Cordillera, southeastern Spain). Chem Geol 197: 55–86

Treloar PJ (1987) The Cr-minerals of Outokumpu – their chemistry and significance. J Petrol 28: 867–886

Vašák S (1981) Geology and mineral deposits relations in Jizera Crystalline Unit abroad Nové Město pod Smrkem. Unpublished MSci. thesis, Faculty of Science, Charles University, Prague, pp 1–101 (in Czech)

Veselý J (1969) Final report of project No. 512 115 020 Svratka Unit. Unpublished MSci thesis, Geoindustria, Prague (in Czech)

Werding G, Schreyer W (1984) Alkali-free tourmaline in the system $MgO–Al_2O_3–B_2O_3–SiO_2–H_2O$. Geochim Cosmochim Acta 45: 1331–1344

Willner AP (1992) Tourmalinites from the stratiform peraluminous metamorphic suite of the Central Namaqua Mobile Belt (South Africa). Miner Depos 27: 304–313